coatings

MDPI

Review

Extreme-Environment Coatings for Offshore Renewable Energy Systems: Coupled Degradation, Testing, and Lifecycle Design

Min Ook Kim

Department of Civil Engineering, Seoul National University of Science and Technology, 232 Gongneung-ro, Nowon-gu, Seoul 01811, Republic of Korea; minookkim@seoultech.ac.kr

Abstract

Offshore renewable energy (ORE) systems experience interacting chemical, biological, and mechanical stresses that make coating performance dependent on component duty and maintenance access. This critical narrative review evaluates conventional and advanced coatings across atmospheric, splash, tidal, and submerged zones, distinguishing laboratory demonstrations from field evidence. Coupled degradation is analyzed in relation to coating architecture: strain-assisted ingress and delamination in organic multilayers; cathodic disbondment in immersed barrier systems; sacrificial consumption in metallic and duplex systems; and wear-induced loss of support in ceramic-rich layers. Surface preparation, layer dimensions, filler dispersion, and wet interfacial properties govern these pathways. Component-specific multi-stressor protocols use matched controls to distinguish interaction from coincident damage. An explicitly illustrative worked example links assumed defect-area histories to a remaining protective life of 2.64 years, repair area, discounted intervention cost, and climate impact. Growth-rate and access-delay scenarios show why these outputs require site calibration and cannot be treated as validated offshore predictions. Qualified multilayer organic and metallic–organic systems remain practical reference options, while nanofillers, self-healing, and sensing functions require demonstrated benefits at matched thickness, cure, and damage state.

Keywords: offshore renewable energy; protective coatings; marine corrosion; coating degradation; multi-stressor testing; service-life prediction; lifecycle design

1. Introduction

The rapid expansion of offshore renewable energy (ORE) is increasing the deployment of fixed and floating offshore wind turbines, wave energy converters, and tidal-current systems in increasingly demanding marine environments. Unlike land-based renewable-energy infrastructure, offshore systems are continuously exposed to combinations of saline moisture, chloride-rich seawater, cyclic wetting and drying, ultraviolet (UV) radiation, temperature variations, waves and currents, suspended particles, and biological activity. These environmental actions can progressively deteriorate structural materials and functional components, thereby affecting reliability, maintenance requirements, and service life [1–3]. Corrosion protection is consequently an integral part of offshore structural design rather than a secondary maintenance consideration [1].

The severity and nature of degradation vary considerably with exposure zone. Atmospheric regions are predominantly affected by salt deposition, humidity, UV radiation, and temperature fluctuations, whereas splash and tidal zones experience repeated wetting–drying cycles, oxygen availability, chloride accumulation, and mechanical impact. Perma-

Check for updates

Academic Editors: Victoria Bustos-Terrones and Ludmila B. Boinovich

Received: 29 August 2026
Revised: 8 October 2026
Accepted: 15 October 2026
Published: 16 October 2026

Copyright: © 2026 by the author. Licensee MDPI, Basel, Switzerland. This article is an open access article distributed under the terms and conditions of the Creative Commons Attribution (CC BY) license.

nently submerged components are additionally subjected to seawater exposure, hydrostatic conditions, biofouling, and microbiologically influenced processes [1,2]. These differences are particularly relevant to offshore renewable-energy devices because a single system may contain structural elements distributed across several exposure zones. Floating systems introduce further complexity through mooring chains, dynamic cables, joints, and other components experiencing simultaneous environmental and cyclic mechanical loading.

Protective coatings constitute one of the principal barriers separating structural substrates from aggressive marine environments. Organic coating systems, particularly epoxy-based systems, are widely employed because of their barrier properties, adhesion, and practical applicability, while metallic and thermally sprayed coatings provide alternative or complementary corrosion protection [1,4]. Hybrid organic–inorganic, ceramic, nanocomposite, and other multifunctional coating concepts have also attracted increasing attention because coating chemistry and microstructure can be engineered to improve barrier performance, mechanical resistance, and functional properties [5]. In practice, coating systems may also be combined with cathodic protection to provide more robust corrosion-control strategies for submerged offshore structures [1,4].

Nevertheless, corrosion resistance alone does not determine long-term offshore coating performance. Biofouling can modify surface characteristics, increase hydrodynamic loads, influence corrosion processes, and complicate inspection and maintenance of offshore renewable-energy infrastructure [3]. Erosion and cavitation are particularly relevant to components subjected to high-velocity water or particle impact, while UV exposure, thermal cycling, mechanical fatigue, and coating–substrate deformation can progressively promote cracking, loss of adhesion, or localized coating failure. Importantly, these degradation processes rarely occur independently under actual offshore conditions. Their interactions can accelerate damage in ways that are difficult to reproduce using conventional single-factor laboratory tests. This discrepancy between laboratory assessment and offshore exposure represents a major challenge in coating qualification and service-life prediction. Current offshore corrosion-protection practices recognize the importance of coating selection, surface preparation, application quality, exposure conditions, inspection, and maintenance [1]. However, laboratory evaluations frequently isolate salt spray, immersion, UV exposure, adhesion, erosion, or mechanical loading. Such approaches are valuable for material screening but may not adequately reproduce the coupled environmental–mechanical stresses experienced during long-term offshore operation. More representative multi-stressor testing and stronger correlations between accelerated laboratory tests and field exposure are therefore required.

Environmental performance is also becoming an important criterion in coating design. Corrosion-protection systems can themselves introduce substances into marine environments through coating degradation, leaching, or sacrificial corrosion processes [6]. At the same time, increasing concern regarding conventional biocidal antifouling technologies has stimulated interest in environmentally benign foul-release surfaces and multifunctional coating strategies. Future offshore coatings must therefore balance corrosion resistance, adhesion, mechanical durability, antifouling performance, maintainability, and environmental compatibility rather than maximizing a single property.

This critical narrative review examines ORE coatings through the connected questions of exposure, coupled failure, qualification, and lifecycle design. Section 2 identifies marine degradation mechanisms and explains how their interactions depend on architecture and exposure. Sections 3 and 4 assess coating technologies, surface preparation, and interfacial performance. Section 5 develops controlled multi-stressor comparisons and field-validation requirements. Section 6 connects condition measurements to remaining useful life (RUL), lifecycle cost (LCC), and lifecycle assessment (LCA), including a worked calculation with

explicitly stated assumptions. Figure 1 summarizes the relationship between exposure zones and layer functions that underpins this analysis.

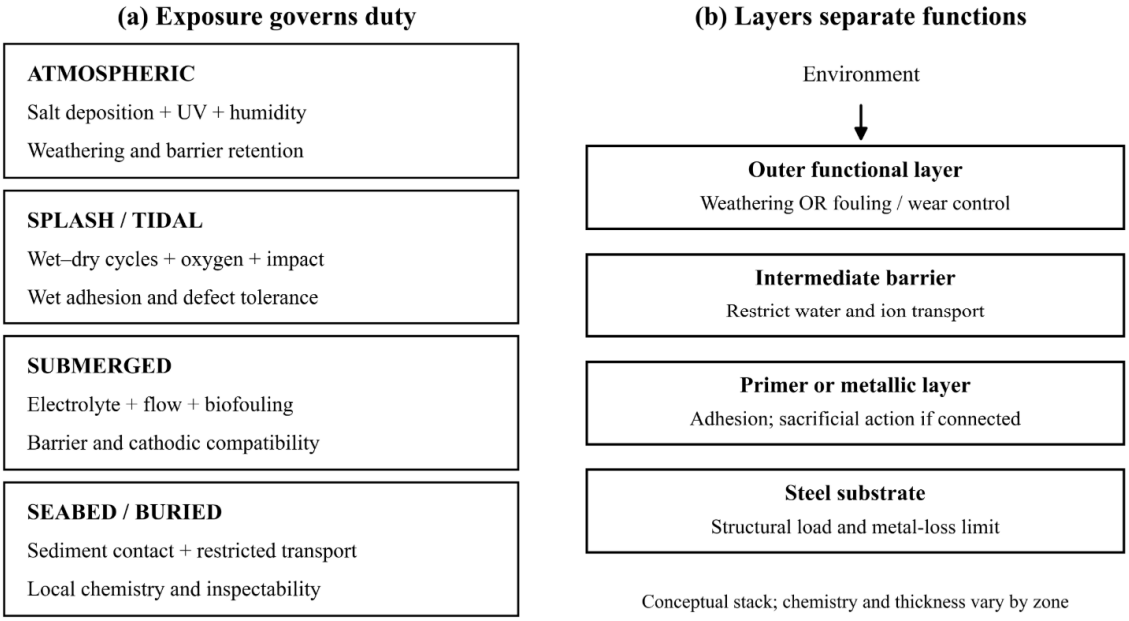


Figure 1. Exposure zones and functional roles within an offshore coating system. (**a**) Principal environmental loads and protection requirements. (**b**) Conceptual layer stack; the primer may provide sacrificial protection only when the material and electrical continuity permit it.

This article is a critical narrative review organized around exposure, coating architecture, coupled degradation, qualification, and lifecycle decisions. Literature identification is selective and relevance-led rather than intended to achieve systematic or exhaustive coverage.

The synthesis prioritizes studies that identify the coating system, substrate, exposure or loading conditions, duration, and a relevant protection endpoint. Offshore exposure studies inform deployment judgments; laboratory studies and evidence from coastal panels, ships, other substrates, or nonmarine environments inform mechanisms only within their stated limits. Reviews provide context, and standards define test or qualification requirements rather than demonstrate field service life. Comparisons consider preparation, thickness, cure, damage geometry, and measurement conditions; heterogeneous results are not pooled into a meta-analysis. This critical narrative review does not provide a registered systematic-review protocol, database-wide search export, exhaustive screening counts, or a formal risk-of-bias score. Selection and publication bias, reliance on accessible English-language records, uneven reporting, and sparse long-term offshore validation may therefore affect the conclusions. Absence from the selected literature is not evidence that a technology lacks field experience, and the classifications in Section 3.5 apply to the cited systems rather than every formulation in a technology family.

2. Marine Exposure and Degradation Mechanisms

ORE systems operate across highly variable marine exposure conditions that impose simultaneous chemical, biological, and mechanical stresses on protective coatings. Offshore structures are commonly divided into atmospheric, splash, tidal, and continuously submerged zones, each characterized by distinct corrosion and coating-degradation processes [1,7]. ISO 12944-9 specifies performance requirements for offshore coating systems in CX atmospheric and Im4 seawater-immersion environments with cathodic protection, including associated splash and tidal exposure [7]. Understanding these zone-dependent

conditions is essential for selecting coating systems capable of maintaining adhesion, barrier performance, and mechanical integrity throughout service.

2.1. Atmospheric, Splash, Tidal, and Submerged Environments

The marine atmospheric zone is not directly immersed in seawater but is continuously influenced by airborne chlorides, high humidity, oxygen, temperature variations, and UV radiation. Salt deposition promotes electrolyte formation when sufficient moisture is present, enabling electrochemical corrosion where coating defects expose the substrate. Simultaneously, UV radiation and thermal fluctuations can induce polymer degradation, discoloration, embrittlement, and microcracking in organic coating systems. Consequently, atmospheric coating systems must combine effective corrosion protection with weathering and UV resistance [1,7].

The splash and tidal zones generally represent the most aggressive regions for coated offshore steel structures. Repeated wetting and drying concentrates chloride salts, while abundant oxygen supports rapid electrochemical reactions. Wave impact, floating debris, suspended particles, and cyclic mechanical stresses further increase the probability of coating damage [8]. Reported corrosion rates for unprotected carbon steel in splash and tidal environments can substantially exceed those under permanent immersion, illustrating the severity of these transitional zones [8]. Cathodic protection may also become intermittent or ineffective above the mean water level, making coating integrity particularly important.

In the continuously submerged zone, persistent seawater contact, dissolved salts, currents, marine organisms, and microbial activity govern coating performance. Coatings are often combined with cathodic protection; the intact coating reduces the steel area that the cathodic-protection system must protect [1,8]. Defects, water uptake, cathodic disbondment, and biological colonization nevertheless remain durability concerns. Moving connections, moorings, dynamic cables, and joints introduce additional interfaces where immersion interacts with cyclic loading.

Exposure descriptions should be accompanied by measurable boundary conditions: time of wetness or immersion duty cycle, temperature, salinity, dissolved oxygen, local flow velocity, and the presence and potential of cathodic protection. A laboratory electrolyte does not reproduce an exposure zone merely because its salt content resembles seawater. Oxygen renewal and deposit coverage can change the cathodic reaction, and splash-zone drying changes both electrolyte continuity and salt concentration. Laboratory–field differences reported by Grinon-Echaniz et al. and Marinova et al. demonstrate why these boundary conditions should be recorded alongside coating rankings [9,10].

2.2. Corrosion, Biofouling, and Microbiologically Influenced Corrosion

Corrosion remains a primary degradation mechanism for metallic ORE components. Once water, oxygen, and chloride ions penetrate coating pores, defects, or damaged regions, localized electrochemical cells can develop at the coating–substrate interface. Progressive underfilm corrosion may subsequently cause blistering, loss of adhesion, delamination, and exposure of larger substrate areas [1,8]. The process is particularly critical at edges, welds, bolts, joints, and mechanically damaged regions where coating thickness or adhesion may be locally inadequate.

Biofouling adds considerable complexity to submerged coating performance. Initial biofilm formation can facilitate subsequent settlement of algae, barnacles, mussels, and other marine organisms. Mature fouling increases surface roughness, hydrodynamic drag, and structural mass and can therefore modify loading and fatigue response [3,11]. These effects are especially relevant to floating structures, mooring systems, dynamic cables, and tidal-energy devices whose performance is closely coupled to hydrodynamic behavior.

Microbiologically influenced corrosion may occur beneath biofilms or deposits when microbial activity changes local oxygen concentration, pH, or electrochemical conditions [8]. Fouling can therefore affect corrosion at defects as well as hydrodynamic loading and inspection access. Biological coverage alone does not establish MIC; the proposed biological mechanism must be linked to localized chemical and corrosion measurements. This distinction supports combining corrosion protection with a separately validated antifouling or foul-release function.

At a defect, anodic metal dissolution is coupled to a cathodic reaction elsewhere on the wetted surface; transport through a pore, along a disbonded interface, or beneath a deposit controls the local reaction environment. Thus, defect width, exposed steel area, and lateral delamination distance are distinct length scales. A small through-thickness defect may be more consequential than a much larger superficial scratch. Biofilm-related oxygen gradients and microbial activity may modify this environment, but surface discoloration or a photograph of fouling cannot establish MIC. Interpretation requires localized corrosion measurements and microbiological/chemical evidence consistent with the proposed mechanism [12,13].

Direct microbial evidence changes the interpretation of a damaged surface. In carbon-steel experiments, mixed sulfate-reducing bacteria (SRB) and total general bacteria produced more severe pitting than SRB alone; the accompanying community supplied locally anaerobic conditions favorable to SRB [12]. However, a 22-month freshwater immersion study of ten stainless steels found severe localized attack on martensitic S40300 without SRB enrichment [13]. The latter is mechanistic evidence from a different substrate and environment, not validation for coated offshore carbon steel. Together, these studies caution against treating SRB abundance or sulfur-rich deposits as a universal MIC diagnosis. A coating experiment should compare abiotic, single-community, and mixed-community conditions while measuring pit development, interfacial chemistry, and coating defects; biological activity and loss of protection must be linked at the same location.

2.3. Erosion, Cavitation, UV Aging, and Mechanical Fatigue

Erosion removes coating material through repeated impact by suspended particles, droplets, or debris. It is relevant to tidal-current rotors, wave-energy devices, leading edges, and other components exposed to energetic flow. Material loss can increase roughness and expose the substrate, after which mechanical removal and corrosion may interact. Flow conditions and material loss must be measured before such an interaction is described as synergistic.

Cavitation represents another severe degradation mechanism for rapidly moving or rotating components. Formation and collapse of vapor bubbles near a coated surface generate localized pressure pulses and repeated impact loading. Once coating damage begins, seawater can penetrate damaged areas and initiate corrosion, potentially creating a coupled cavitation–erosion–corrosion process. Such interactions are especially important for ocean-energy devices containing blades, bearings, seals, and other moving components [14]. Above and near the waterline, UV exposure and thermal cycling contribute to aging of polymeric coatings. Photo-oxidation can alter polymer chemistry and gradually reduce flexibility and mechanical properties, whereas temperature fluctuations generate expansion–contraction cycles within the coating/substrate system. Differences in thermal and mechanical properties between layers may promote interfacial stresses, cracking, or delamination [15].

Mechanical fatigue further compounds these effects. Offshore wind towers and foundations experience cyclic wind and wave loading, while floating platforms, moorings, and wave- and tidal-energy devices undergo persistent dynamic motion. Local coating cracking

can expose steel surfaces, after which corrosion may accelerate fatigue deterioration of the substrate [1]. Thus, coating mechanical integrity is closely connected to structural durability rather than functioning solely as a corrosion barrier.

Erosion and cavitation should also be distinguished by loading conditions and damage metrics. Particle erosion depends on particle size, concentration, hardness, impact angle, and impact velocity; cavitation depends on local pressure relative to vapor pressure and the dynamics of bubble collapse. The relevant coating scales include thickness, pore/defect dimensions, and the size of the impact-affected region. A hard layer can resist cutting yet fail by brittle cracking, whereas a compliant layer may accommodate deformation but suffer wear or interfacial fatigue. Report mass or volume loss together with exposed area, duration, and thickness, and examine whether corrosion contributes to material removal. An offshore-oriented study of thermally sprayed aluminum modified by plasma electrolytic oxidation illustrates the need to compare corrosion, wear, and their coupled response rather than infer tribocorrosion resistance from hardness alone [16].

Experiments also show why flow and material identity must remain explicit. Natural-seawater impingement tests on bare marine carbon steel found little change in flow-accelerated corrosion rate between 5 and 8 m/s under a relatively compact rust layer, while sand impact altered erosion–corrosion and pit-boundary removal [17]. This describes exposed substrate after barrier loss, not a safe velocity limit for a coating. TiAlN-coated high-speed steel showed little upstream coating failure but damage on the downstream face, where localized flow and turbulence promoted cracking and layerwise spallation [18]. A nominal flow velocity therefore cannot rank coatings without geometry and particle conditions. In seawater ultrasonic cavitation tests, carbon-nanofiber-reinforced polyurethane formulations differed from unreinforced polyurethane and commercial comparison coatings [19]. Such laboratory erosion metrics should be paired with wet adhesion and cyclic-strain tests before selection for tidal blades.

2.4. Coupled Multi-Stressor Degradation

Coupled degradation occurs when one process changes the rate-controlling conditions or resistance governing another process. Coexistence alone is insufficient: chloride exposure and cyclic strain are coupled when a strain-induced crack changes electrolyte access, or when water uptake reduces the interfacial resistance against crack growth. The useful mechanistic variables are therefore transport-path connectivity, local pH and potential, wet mechanical properties, interfacial fracture resistance, and evolving defect geometry. These variables provide the link between the damage modes described above and the observations needed to distinguish their interactions [9,16,20–22].

A first feedback loop links water uptake, mechanical damage, and underfilm corrosion. Water can plasticize a polymer and weaken interfacial interactions; differential swelling and repeated substrate strain then promote cracks or interfacial separation. The resulting short transport paths accelerate electrolyte access to exposed steel. Anodic iron dissolution produces ferrous ions, while oxygen reduction at accessible cathodic regions produces hydroxide. Hydrolysis near anodic sites and alkalinization near cathodic sites create spatially different chemical conditions. Where retained, corrosion products can exert wedging stresses beneath a partially detached coating, enlarging the wetted interface and increasing subsequent mechanical damage. This feedback is a mechanism to test, not an inevitable result of every deformation. Stress-corrosion experiments on epoxy zinc-rich systems indicate mechanical–electrochemical interaction [22], whereas the compression study in [21] found no reduction in protection in plastically deformed regions under its tested conditions. Damage mode, coating architecture, and strain history determine whether the feedback is activated.

A second coupling involves cathodic protection and adhesion. Polarizing exposed steel suppresses anodic dissolution, but oxygen reduction and, at sufficiently negative potentials, water reduction can increase interfacial alkalinity; hydrogen evolution may also become relevant. If water and ions can reach a susceptible coating–steel interface, these conditions can promote cathodic disbondment. Thus, stronger polarization does not necessarily preserve coating adhesion, and coating compatibility must be evaluated together with the potential relative to a named reference electrode. Deposits, shielding, and local electrolyte access can make the response spatially nonuniform. The material-specific balance between steel protection and coating disbondment motivates paired polarized/unpolarized tests [4,9,23].

A third coupling links erosion or cavitation to electrochemical and interfacial damage. Repeated impact removes polymer, oxide, or corrosion products, exposes fresh reactive material, and increases electrolyte renewal. Corrosion can then undercut a metallic layer or weaken support beneath a wear-affected region, increasing subsequent mechanical loss. The oxide-modified TSA study of López-Ortega et al. provides a relevant experimental comparison of corrosion, wear, and tribocorrosion [16]. Biofouling adds another route by modifying oxygen transport and local chemistry while changing roughness and hydrodynamic loading. These effects need not all accelerate corrosion: transport-blocking deposits can reduce a reaction while differential aeration intensifies localized attack. Biological presence should therefore be linked to measured local conditions rather than assigned an automatic synergy [3,8,11].

Coupling strength must be defined for a specified response and baseline. For additive material loss, the interaction residual is $S = L_{AB} - L_A - L_B + L_0$, where L_{AB} is the loss under combined exposure and L_A, L_B, and L_0 are the isolated-stressor and baseline losses over the same area and duration. Positive S indicates excess loss relative to that additive baseline, subject to uncertainty and comparable boundary conditions. ASTM G119 provides wear–corrosion accounting for metallic materials in liquids or slurries [24]. Retained corrosion products, different measured materials, or changing exposed areas can invalidate a simple mass balance. Delamination and impedance instead require an appropriate response model; logarithmic impedance values are not additive material losses.

Architecture and exposure dependence. Figure 2 distinguishes five candidate failure pathways. These are mechanistic interpretations of the reviewed evidence, not a numerical ranking of coupling coefficients. The dominant pathway is the one that controls the first loss of the required function under the specified duty; it can change as defects grow, sacrificial material is consumed, or the environment changes.

Organic multilayers. For epoxy barriers with a weather-resistant polyurethane finish, atmospheric aging can reduce surface integrity, while strain at welds, edges, or repairs opens transport paths. In the splash/tidal zone, recurrent hydration and oxygen replenishment can strengthen the feedback between cracking, wet-adhesion loss, and underfilm corrosion. The feedback is weaker when the film remains continuous and the interface retains wet fracture resistance. A zinc-rich primer introduces a further condition: electrically connected zinc can protect exposed steel while sufficient active material remains, whereas poorly connected or depleted pigment cannot be assumed to arrest underfilm attack. EIS loss, lateral delamination, and primer consumption therefore represent different stages rather than interchangeable measures of failure [4,10,20–22].

Immersion barriers with cathodic protection. At a holiday in an immersed epoxy system, cathodic polarization can suppress steel dissolution while promoting alkaline conditions at an electrolyte-accessible interface. The resulting competition makes disbonded area a necessary endpoint alongside steel loss. A susceptible wet interface and increasingly negative potential can favor disbondment, whereas an intact, well-bonded barrier limits

lateral access. Thus, a system can show little metal loss but substantial coating separation. Splash-zone comparisons must account for intermittent electrical protection during wetting; fully immersed, continuously polarized tests cannot represent that duty without modification [4,9,23].

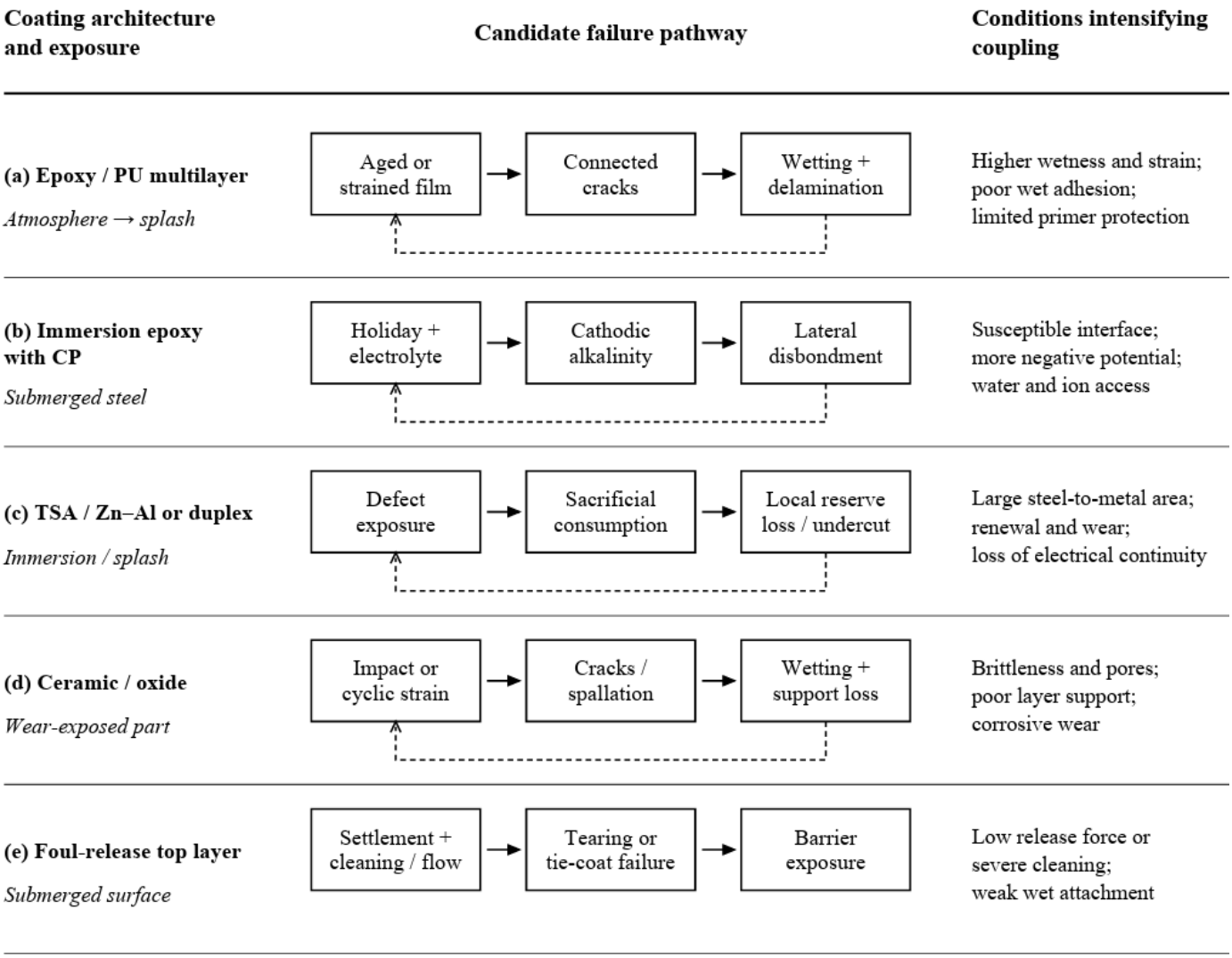


Figure 2. Architecture-dependent coupled failure pathways and conditions expected to intensify them. Return arrows indicate possible feedback from interface or support loss to further damage; arrows do not encode a measured rate. Sacrificial protection can interrupt the transition from coating damage to steel corrosion. The foul-release pathway reaches corrosion only after failure of the underlying barrier.

Metallic and duplex architectures. TSA or Zn–Al layers can retain local protection after barrier damage because the connected metallic coating supplies sacrificial current. Coupling initially concerns defect exposure, metallic consumption, and deposit formation rather than immediate steel corrosion. For an organic-over-metal duplex system, the overcoat reduces electrolyte access and electrochemical demand; local overcoat loss can concentrate that demand around a defect. A larger exposed-steel area relative to the available connected metal, coating removal by wear, or loss of continuity can shift the controlling pathway toward reserve depletion and substrate exposure. Grinon-Echaniz et al. found an exposure-dependent ranking: Al-based coatings favored immersion, whereas Zn–15Al performed better in atmospheric/splash exposure [9]. This evidence precludes assigning one coupling strength to all sacrificial systems [4,9,20].

Ceramic-rich and oxide-modified layers. Under impact or cyclic deformation, connected pores, brittle cracking, and inadequate support can convert local surface wear into electrolyte access and interfacial undercutting. Continued loading then removes the weakened layer. This wear–corrosion feedback should be evaluated separately from hardness: an intact hard surface may resist cutting, but a cracked or poorly supported layer can spall. The oxide-modified TSA architecture retains an underlying sacrificial layer and should not be equated with a stand-alone ceramic coating on steel. Its relevant endpoints include coating volume loss, remaining metallic thickness, fracture location, and substrate attack [16,18].

Foul-release and compliant outer layers. For a silicone or compliant polyurethane surface over an anticorrosive barrier, settlement and cleaning can alter roughness, adhesion, and mechanical loading. Insufficient release force can leave fouling in place; excessive cleaning or poor wet attachment can tear the top layer or detach it at the tie coat. Corrosion becomes a downstream consequence only if the underlying protective barrier is also compromised. Biofilm-modified chemistry can increase or decrease local reaction rates and requires separate biological controls. Favorable static-panel performance has also been reported, so low flow does not by itself establish failure of a foul-release system [3,8,25,26].

Nanofillers, inhibitors, and healing functions modify these pathways rather than define a single additional failure class. Well-dispersed fillers can restrict connected transport, while agglomerates or weak filler–matrix interfaces can increase strain-assisted ingress. Active inhibitors may reduce corrosion at an accessible defect without restoring adhesion, and polymer healing requires adequate mobility and contact between damaged surfaces. Their effect on coupling must therefore be tested against the same parent architecture, thickness, cure, and defect geometry, using the limiting wet endpoint rather than the presence of an added function [27–32].

A practical comparison of coupling strength uses a common damage response D, measured at a fixed time, within each architecture and exposure zone. For a balanced two-stressor experiment with binary indicators A and B, an additive response model gives the interaction contrast in Equation (1). Here D is defined so that a larger value means more damage; the bars denote replicate means. The contrast is a statistical effect on the chosen response scale, not proof of a mechanism or a transferable material constant.

$$\beta_{AB} = \overline{D}_{11} - \overline{D}_{10} - \overline{D}_{01} + \overline{D}_{00} \quad (1)$$

For example, use delaminated area for wetting–strain interaction, disbondment radius for polarization–strain interaction, or substrate loss for wear–corrosion. Report the contrast, its confidence interval, endpoint units, and exposure duration for each coating/zone combination. A comparison across architectures requires the same endpoint and damage geometry; otherwise only the mechanism, not the numerical magnitude, can be compared. Bounded area fractions may require a generalized model, in which case interaction depends on the selected link scale. The available heterogeneous studies support the directional comparisons above but do not provide a defensible pooled coefficient. The matched experiments in Section 5.3 are intended to resolve this gap.

Inspection locations should follow the component duty. Offshore wind steel requires assessment of splash-region rust propagation, biological coverage, blistering, and submerged defects. Wave-energy devices additionally require attention to wear and joints or fasteners; tidal devices require blade-edge, hub, and bolt-interface assessment. Crevices, welds, and disbonded coating edges are recurrent targets on support steel. These are inspection priorities derived from published mechanisms and exposure studies, not original field observations from the present critical narrative review [3,4,9,10,14,16,20].

Failure diagnosis must distinguish mechanisms with different necessary conditions. Galvanic attack requires dissimilar conductive materials, an electrical connection, and an electrolyte. MIC involves biological modification of corrosion conditions and requires independent confirmation. UV aging changes the exposed polymer surface; thermal cycling imposes strain through expansion mismatch; osmotic blistering involves water transport and an osmotic gradient; and stress-corrosion cracking concerns a susceptible substrate under tensile stress in a specific environment. A cracked paint surface alone does not diagnose substrate stress-corrosion cracking. Similarly, cavitation is a plausible diagnosis only where local operating pressures support bubble formation and collapse. Field exposure and post-exposure characterization are necessary to distinguish these alternatives [1,4,8,9,14,20].

3. Coating Technologies for Offshore Renewable Energy

Protective coatings for ORE infrastructure must retain their required functions under seawater exposure, biological activity, erosion, and cyclic loading. Selection therefore depends on corrosion resistance, wet adhesion, mechanical integrity, fouling response, repairability, and exposure zone. The following comparison treats the complete coating architecture as the unit of qualification, including any active or functional layer.

3.1. Organic and Polymeric Coatings

Organic coatings remain the most widely used protective systems for offshore steel structures because they provide an effective physical barrier against water, oxygen, and chloride penetration while offering relatively simple application and repair. Epoxy coatings are particularly important because of their strong adhesion, chemical resistance, and compatibility with corrosion-inhibiting pigments and fillers [1,4]. Polyurethane layers are frequently employed as topcoats where improved UV stability, flexibility, and weathering resistance are required. Multilayer systems typically combine complementary functions, for example, a zinc-rich primer for sacrificial protection, an epoxy intermediate layer for barrier performance, and a polyurethane topcoat for environmental resistance. Field investigations have demonstrated that properly designed multilayer and duplex systems can retain considerable protective capability under offshore exposure, although local mechanical damage may initiate delamination and subsequent substrate corrosion [20]. Organic coatings therefore remain attractive for atmospheric and splash-zone components, but their long-term performance depends strongly on surface preparation, coating thickness, curing quality, adhesion, and defect control [4,20].

Thickness must be reported for each coat and for the complete system. In the monopile experiments of Marinova et al., the nominal atmospheric systems were 280–460 µm thick, including examples with a 60 µm zinc-rich epoxy primer, a 160–170 µm epoxy intermediate coat, and a 50–60 µm polyurethane topcoat. Splash-zone systems were 600–660 µm nominally, whereas immersed systems were 350–600 µm [10]. The measured thicknesses differed from the nominal specifications; for example, an atmospheric 280 µm system measured 399 µm, and a splash-zone 660 µm system measured 821 µm. These differences matter when interpreting comparative durability. Greater thickness can lengthen an intact transport path, but excessive build can also impair cure, retain solvent, or increase shrinkage stress. Results should therefore be compared using measured layer thickness, cure state, and defect population, not resin name alone.

Critical assessment and outlook. Qualified multilayer organic systems remain the practical reference for large atmospheric and splash-zone steel because their application and field behavior are comparatively well documented [4,10,20]. The priority should be retention of wet adhesion and strain tolerance at edges, welds, and realistic defects. A

polyurethane finish adds value where weathering governs, but its presence alone does not improve an immersed barrier. For severe splash exposure with delayed repair, compare an epoxy system with a qualified duplex alternative using damaged specimens and actual preparation quality. The most useful development is a reproducible extension of the maintenance interval, not a higher initial dry-film property obtained through uncontrolled extra thickness.

3.2. Metallic, Ceramic, and Hybrid Coatings

Metallic coatings provide an alternative protection mechanism by combining barrier effects with sacrificial electrochemical protection. Zinc, aluminum, and Zn–Al alloys are widely applied to offshore steel through thermal spraying or related metallization processes [33]. Thermally sprayed aluminum (TSA) and zinc–aluminum systems are particularly attractive for aggressive marine environments because, under suitable electrochemical conditions, they can protect steel around localized defects. Recent reviews have discussed the importance of Zn- and Al-based sacrificial coatings for offshore wind structures, although their effectiveness depends strongly on coating composition, porosity, thickness, sealing, and substrate preparation [33].

Combining metallic coatings with organic layers produces duplex systems, in which sacrificial protection from the metallic layer is complemented by the barrier properties of the polymeric topcoat. Offshore field exposure has shown particularly favorable corrosion protection from Zn/Al metallization combined with epoxy and polyurethane layers [20]. Such systems are promising for components requiring extended maintenance intervals.

Ceramic coatings and ceramic-containing layers offer high hardness, thermal stability, chemical resistance, and resistance to erosion and wear. Their intrinsic brittleness and differences in mechanical behavior relative to steel, however, can restrict their use on dynamically loaded components. Organic–inorganic hybrid coatings provide an alternative approach by integrating the flexibility and processability of polymers with the barrier, mechanical, or chemical properties of inorganic phases [5]. Sol–gel-derived and other hybrid architectures are therefore of growing interest where simultaneous corrosion resistance, adhesion, and mechanical durability are required.

For metallic coatings, coating thickness defines the available sacrificial material as well as the barrier path, while connected porosity and electrical continuity determine how the layer actually protects steel. Grinon-Echaniz et al. examined approximately 300 µm thermal-spray layers with artificial defects exposing 5% of the surface area; Eom et al. used a 100 µm Zn–Al layer, both alone and beneath epoxy [4,9]. These are different architectures and should not be combined into a single thickness–lifetime relationship. Splats, oxide boundaries, pores, and the ratio of exposed steel to surrounding metallic coating control local electrochemical demand. A sealer can limit connected pathways, but its penetration and compatibility must be distinguished from the thickness and function of a separately qualified organic overcoat.

Damage tolerance of TSA has been measured under defined electrochemical conditions. Paul exposed wire-arc-sprayed 1050 Al on carbon steel with approximately 5%–18% deliberately exposed steel area to synthetic seawater at 25 °C for 420 days. Steel potentials remained below −800 mV versus Ag/AgCl even at the largest tested holiday fraction, and initial damage effects did not produce a significant overall performance penalty over that experiment [34]. This supports a laboratory damage-tolerance mechanism; it does not establish an allowable 18% defect fraction in a design, a universal polarization criterion, or a 20–25-year lifetime. Available aluminum, deposit formation, water renewal, and electrical continuity must still be checked for the intended site.

"Ceramic" likewise describes composition rather than one-dimensional regime. A thin conversion or sol–gel-derived oxide/hybrid film, a deposited ceramic-rich layer, and a plasma-electrolytically oxidized metallic coating have different supporting architectures and strain capacities. López-Ortega et al. specifically evaluated an oxide-modified thermal-spray aluminum system for submerged components [16]; its performance should not be transferred to a stand-alone ceramic film on steel. For thin hybrid films, local substrate relief and pinholes may approach or exceed the film thickness, whereas a thicker ceramic-rich deposit can develop residual and cyclic stresses across its thickness. Researchers should report the functional-layer thickness, supporting-layer thickness, pore size, and crack dimensions separately. The appropriate scale is set by coverage, strain accommodation, and wear depth rather than hardness alone [5,9,16].

The ceramic comparison is also process-specific. In an experimental comparison of alumina-based coatings, HVOF spraying of fused-and-crushed powders gave the highest abrasion, erosion, and cavitation resistance among the tested deposits, while the benefit of nanostructured feedstock depended on using the plasma-spray route [35]. This does not establish that every ceramic coating outperforms a compliant polymer under seawater impact. In PDMS-based polyurethane, increasing the PDMS fraction improved laboratory cavitation resistance while reducing adhesion [36]. The competing response makes retained attachment, supporting-layer compliance, and defect growth as important as material-loss resistance. For large strained ORE components, wear protection should therefore be localized and validated with the complete coating stack.

Critical assessment and outlook. Metallic–organic duplex systems are strong candidates for inaccessible steel where qualified fabrication can combine a continuous barrier with local sacrificial protection; the three-year offshore evidence supports this preference more directly than short immersion tests on novel films [9,20]. Selection between Zn-rich and Al-rich architectures remains zone- and formulation-dependent, and additional sacrificial material introduces consumption and release burdens. Ceramic-rich layers should be targeted to localized wear duty and qualified under wet cyclic strain; they are a weaker default choice for large, deforming structures. Hybrid films are most credible as adhesion-promoting or barrier-modifying parts of a complete coating stack until comparable field evidence establishes stand-alone durability [5,16,33].

3.3. Nanocomposite and Multifunctional Coatings

Nanocomposite coatings contain nanoscale fillers that modify transport, interfaces, mechanical response, or surface function within a polymeric or hybrid matrix. The examples considered here include PANI/ZrO_2-modified epoxy and modified acrylic resin containing functionalized carbon nanotube/silica fillers. A well-dispersed filler may lengthen electrolyte transport paths; the benefit depends on dispersion, matrix continuity, and the absence of connected interfacial voids [27,28].

The potential value of nanocomposites lies in changing a specific limiting mechanism, such as connected porosity, filler–matrix debonding, or inhibitor delivery. Recent polymer nanocomposite systems combine barrier modification with corrosion-inhibiting or antifouling functionality, including PANI/ZrO_2-modified epoxy [27] and PAZ/N-PMI-modified acrylic coatings containing functionalized carbon nanotube/silica fillers [28]. However, a higher initial impedance or water contact angle cannot establish an offshore advantage unless thickness, cure, and defect geometry are controlled. Dispersion and interfacial compatibility govern whether a filler blocks a transport path or creates a new one; they must be treated as distinct, measurable design variables.

A nanocomposite is not necessarily a nanometre-thick coating. The nanoscale descriptor refers to an additive or internal structure; the applied protective film can remain a

conventional micrometre-scale layer. Report filler dimensions and morphology, agglomerate size, loading, and dry-film thickness separately. Evaluate transport changes together with filler distribution and coating continuity, because agglomeration or poor interfacial wetting may introduce defects rather than improve protection. Conductive fillers also require attention to electrical connectivity and contact with exposed metal rather than an assumption that greater conductivity always improves protection. Comparisons should include the unfilled matrix at matched thickness and cure, so that a change in barrier performance can be attributed to the filler architecture [27,28].

Filler morphology, agglomeration, and interfacial wetting influence the continuity of the cured coating. The PANI/ZrO_2 and functionalized nanotube/silica systems illustrate distinct filler architectures, while the silica/epoxy study demonstrates a loading-dependent optimum [27–29]. These results support evaluating each formulation separately. Cross-sectional particle distribution, agglomerate size, and connected voids should be examined after curing and aging. Comparisons should determine whether changes in filler loading improve barrier continuity or instead produce resin-poor regions and interfacial defects; a beneficial loading in one formulation should not be transferred to another without testing.

Interfacial compatibility determines whether the filler–polymer boundary transfers load or becomes a preferential water pathway. Suitable surface chemistry can improve wetting and bonding; for example, an amino-functional silane can couple a hydroxylated silica surface to an epoxy network where the curing chemistry permits. Weakly bonded or poorly wetted surfaces can debond during swelling and cyclic strain, creating electrolyte-accessible interfacial gaps. Conversely, a highly polar surface treatment may aid aqueous dispersion while increasing water affinity, so dispersion quality and water uptake must be tested separately. Fan et al. studied modified silica of approximately 800 $\pm$ 50 nm in waterborne epoxy and found the best tested corrosion response at 3 wt.% rather than at higher loading [29]. These are submicrometre fillers, not proof of a nanoscale optimum; the result illustrates the formulation-specific balance between void filling, interfacial chemistry, and agglomeration.

Critical assessment and outlook. A convincing nanocomposite comparison should include unfilled resin, untreated filler, and surface-treated filler at the same loading, measured thickness, and cure. Report cross-sectional agglomerate size/distribution, cure conversion or glass-transition behavior, water uptake, wet adhesion, and impedance after damage and aging. Electrically conductive fillers require additional checks for contact with exposed steel and unintended cathodic activity. This critical narrative review favors additives that demonstrably slow the dominant wet failure process at practical application viscosity; a formulation that improves one short-term electrochemical metric but reduces strain tolerance or repair compatibility should not replace the qualified reference coating [27–29].

3.4. Antifouling, Self-Healing, and Smart Coatings

Antifouling coatings are particularly relevant to continuously submerged components, including floating foundations, mooring systems, dynamic cables, wave-energy devices, and tidal turbines. Conventional antifouling coatings often rely on controlled release of biocidal compounds, whereas the approaches discussed here include silicone-based foul-release surfaces, engineered microtopographies, and multifunctional polyurethane composites. These strategies aim to reduce settlement or facilitate removal. Lower environmental impact must be demonstrated using formulation-specific release, toxicity, durability, and maintenance evidence.

Self-healing coatings represent a further transition from passive to active protection. Damage-responsive systems can incorporate corrosion inhibitors within micro- or nanocontainers or employ reversible chemical and physical interactions that enable closure or repair of microcracks. Recent marine polyurethane systems based on reversible hydrogen-bond

interactions have demonstrated simultaneous self-healing and antifouling capability [30]. Similarly, multifunctional nanocomposite coatings have been developed to integrate corrosion protection, antifouling behavior, and self-healing within a single material [28].

In inhibitor-based protection, coating damage admits electrolyte and local corrosion changes pH or ion concentration. A responsive shell or gate then changes permeability, releasing the stored inhibitor, which must diffuse to and adsorb or react at the active metal surface before it is lost to the surrounding water. Shchukin et al. demonstrated pH-triggered benzotriazole release from polyelectrolyte-based nanocontainers in a hybrid coating on an aluminum alloy [31]. That is active inhibition at a defect, not necessarily closure of the polymer crack, and it cannot be transferred quantitatively to offshore steel. More directly for mild steel, Qian et al. used polydopamine-gated mesoporous silica in a waterborne alkyd coating: acidic conditions promoted inhibitor release, while dopamine-related interactions with iron oxides provided a second protective contribution [32].

Intrinsic healing requires damaged polymer surfaces to approach and regain molecular connectivity. In a reversible hydrogen-bond network, bond exchange and chain motion can reconnect contacting surfaces, but cooling, extensive cross-linking, contamination, or a wide material-loss gap can prevent recovery. Cui et al. reported 85% recovery of tensile strength after 48 h at room temperature for their polyurethane composite; heating accelerated recovery [30]. That number describes the reported mechanical metric and conditions, not proven underwater recovery of an ORE corrosion barrier. Rupture-release capsules provide a different route through delivery and curing of a repair agent, but the locally consumed reservoir is finite. All such systems must be evaluated against flow-driven washout, seawater chemistry, damage size, and repeated events.

Smart coatings should distinguish physical-damage detection, corrosion sensing, active inhibition, and restoration of a barrier. These functions have different triggers and outputs. A mechanically ruptured container may release a marker before metal corrosion begins; a corrosion-sensitive molecule instead responds to a local chemical change after electrolyte reaches the substrate. A visible response does not establish that the coating has healed. Multifunctional marine coating demonstrations, including the system reported by Wang et al., motivate this distinction, but their claimed functions require separate verification under the intended service conditions [37].

For a corrosion-responsive sensor, the sequence is electrolyte ingress, electrochemical reaction, local chemical change, and an optical or electrical response. At a cathodic region, hydroxide production can activate a pH-sensitive color probe; near an anodic site, dissolved metal ions can provide a different chemical trigger. Wang et al. demonstrated a pH-responsive microsphere coating in which pink coloration developed near cracks as local pH increased, and the time-dependent width of that region was compared with electrochemical evidence for different healing systems [38]. Such a signal maps the evolving reaction environment, not crack depth or metal loss directly. Under seawater, background pH, buffering, indicator leaching, illumination, turbidity, and overlying fouling may change signal contrast and response time. Calibration must separate mechanical damage, corrosion initiation, and later healing, including false-positive controls and a demonstrated route for remote readout.

A calibrated sensing response can precede visible metal damage without measuring damage depth directly. Zhang and Frankel detected color or fluorescence changes in an acrylic indicator coating at cathodic charge equivalent to dissolution of a hemispherical pit approximately 10 μm deep [39]. This was a charge-based sensitivity comparison, not direct optical measurement of a 10 μm pit. Response time depended on pH sensitivity rather than coating protectiveness. For an underwater warning system, the development target should therefore be a validated detection threshold, false-alarm rate, and readable signal under fouling, together with evidence that the indicator does not weaken the primary barrier.

For foul-release coatings, outer-surface chemistry, texture, film thickness, and compliance act together. Reducing attachment strength is distinct from preventing settlement, and release also requires sufficient hydrodynamic or cleaning force. A coating that releases fouling on a moving hull may retain organisms on a slowly moving platform or sheltered foundation [25]. Engineered microtopography introduces an additional length scale: Schumacher et al. investigated engineered polydimethylsiloxane topographies with 2 µm feature spacing and found reduced Ulva zoospore settlement relative to a smooth control, with the response depending on geometry and engineered roughness [40]. Thus, a texture that discourages one organism cannot be assumed to prevent mixed-community fouling. Feature width, height, spacing, organism size, and retention of texture after abrasion should be reported in addition to contact angle.

The evidence does not support ruling out foul-release coatings on all stationary structures. Lagerström et al. compared one silicone foul-release coating with two copper-containing coatings on static panels at three Baltic locations over one year; the silicone system performed as well as or better than the copper systems in that study [26]. This counterexample qualifies the moving-hull argument, while its geographical and formulation limits prevent universal transfer to offshore foundations. Selection should consider the local community, seasonal settlement, cleaning access, adhesion of the soft layer, and mechanical wear, rather than using either water contact angle or vessel speed as a sufficient performance criterion.

Active features must also fit within the protective film. Nanocontainers and micrometre-scale capsules should remain embedded without generating connected voids, and their loading must not impair application or cure. Report capsule/container dimensions, damage width and depth, release or healing time, temperature, immersion chemistry, and the number of repeated damage events. Recovery should be measured against both the intact and damaged states using barrier response, wet adhesion, and local corrosion activity; scratch disappearance or tensile-strength recovery alone does not demonstrate recovery of corrosion protection [28,30–32].

Critical assessment and outlook. Foul-release is most attractive where a smooth, compliant surface survives wear and available flow or gentle cleaning can detach organisms; sheltered static regions require direct validation [25,26]. Self-healing and sensing functions offer useful supplementary protection, but a limited inhibitor reservoir or an optical warning obscured by fouling is not a substitute for a durable primary barrier. For inaccessible submerged steel, the near-term preference is a qualified barrier plus compatible cathodic protection, with active additives admitted only after their effect on permeability, wet adhesion, repeated damage, release, and detection has been established. Table 1 summarizes the technologies; Table 2 reports representative dimensional evidence.

Table 1. Comparison of protective coating technologies, protection mechanisms, advantages, limitations, and potential applications in offshore renewable-energy systems.

Coating Type	Typical Materials/ Systems	Main Protection Mechanism	Key Advantages	Main Limitations	Suitable Offshore Exposure/ Application	Refs.
Organic/ polymeric	Epoxy, polyurethane, zinc-rich epoxy, multilayer epoxy/PU	Physical barrier against H_2O, O_2, and Cl^-; inhibition or sacrificial action with zinc-rich primers	Good adhesion; chemical resistance; easy application and repair; mature technology	Water uptake, UV aging, cracking, delamination; sensitivity to surface preparation and defects	Atmospheric and splash zones; towers, transition pieces, foundations	[1,4,20]

Table 1. *Cont.*

Coating Type	Typical Materials/ Systems	Main Protection Mechanism	Key Advantages	Main Limitations	Suitable Offshore Exposure/ Application	Refs.
Metallic	TSA, TSZ, Zn–Al alloys, hot-dip galvanized Zn	Barrier and sacrificial protection of steel	Long-term corrosion protection; tolerance to localized damage; high mechanical robustness	Porosity; possible sealing requirement; application cost and process constraints	Splash, tidal and submerged zones; foundations and structural steel	[20,33]
Duplex systems	Zn/Al metallization + epoxy intermediate coat + polyurethane topcoat	Sacrificial metallic protection combined with polymeric barrier protection	Complementary barrier and sacrificial protection; potential for longer maintenance intervals	Multistep application; interlayer compatibility and quality control required	Highly aggressive offshore zones, particularly splash-zone structures	[20,33]
Ceramic/ inorganic	Thermally sprayed alumina-based ceramics; oxide-modified TSA	Hard or oxide surface layers; barrier and wear response depend on porosity and coating support	Potentially high hardness and wear resistance; performance depends on porosity, support and strain compatibility	Brittleness; possible cracking and poor strain compatibility with steel	High-wear components; tidal and wave-energy components exposed to erosion	[16,35]
Organic–inorganic hybrid	Sol–gel hybrids, polymer–silica, polymer–ceramic architectures	Combined polymer barrier and inorganic reinforcement	Improved barrier properties, adhesion, mechanical durability and tunable functionality	Processing complexity; scale-up and long-term offshore validation remain limited	Atmospheric, splash and submerged components requiring multifunctional protection	[5]
Nano-composite	PANI/ZrO_2-modified epoxy; functionalized CNT/silica-filled acrylic systems	Tortuous diffusion pathways, passivation, hydrophobicity and/or reinforcement	Improved corrosion response in tested formulations; combined anticorrosion–antifouling functions	Nanoparticle agglomeration; dispersion sensitivity; uncertain large-scale durability	Broad potential across splash and submerged environments	[27,28]
Antifouling/ foul-release	Biocidal coatings; silicone/PDMS foul-release surfaces; engineered micro-topographies; polyurethane composites	Prevents settlement, inhibits organisms, or reduces adhesion strength of marine growth	Reduced settlement or attachment in tested systems; benefits depend on organism and exposure	Biocide toxicity concerns; gradual depletion; durability of foul-release surfaces	Continuously submerged surfaces, floating structures, moorings and tidal devices	[3,25,26,30,40]
Self-healing	Microcapsule/ container systems, reversible polymer networks, inhibitor-releasing coatings	Autonomous closure of defects and/or release of corrosion inhibitors	Potential recovery of barrier or inhibition functions after damage; field repair benefit requires validation	Limited healing cycles; triggering requirements; manufacturing complexity	Damage-prone submerged and splash-zone components	[28,30,31]

Table 1. *Cont.*

Coating Type	Typical Materials/ Systems	Main Protection Mechanism	Key Advantages	Main Limitations	Suitable Offshore Exposure/ Application	Refs.
Smart/sensing	Damage-indicating fluorescent fillers; thermally responsive shape-memory epoxy; pH-responsive indicators	Indicates mechanical damage or corrosion-related pH changes; heat may enable shape recovery	Early warning in laboratory demonstrations; heat-assisted recovery in suitable formulations	Cost, sensor stability, offshore validation and integration challenges	High-value or difficult-to-access offshore components	[37–39]
Multi-functional coatings	Anticorrosion + antifouling + self-healing/sensing nanocomposites	Multiple coupled protective mechanisms within one coating architecture	Combines selected protective functions in laboratory demonstrations; offshore durability requires validation	Complex formulation; competing functions; scalability and environmental qualification	Future ORE systems exposed to coupled corrosion, fouling and mechanical damage	[27,28,30,37]

Table 2 consolidates reported coating dimensions and distinguishes nominal specifications from measured values. These examples support comparisons of architecture; they are not general minimum thicknesses or guaranteed service-life specifications.

Table 2. Reported dimensions of selected offshore coating systems and their interpretation.

System and Source	Reported Dimensions	Interpretation for Comparison
Atmospheric paint systems [10]	Nominal total: 280–460 µm. Examples: primer 60 µm; epoxy 160–170 µm; topcoat 50–60 µm.	Compare constituent layers and measured build. A 280 µm nominal system measured 399 µm.
Splash-zone paint systems [10]	Nominal total: 600–660 µm. Measured totals: 629–821 µm.	High build provides barrier/wear reserve; measured thickness, cure and defects remain essential.
Submerged paint systems [10]	Nominal total: 350–600 µm. Measured totals: 435–629 µm.	Immersion and cathodic compatibility must be evaluated at the actual thickness.
Zn–Al and duplex coatings [4]	Zn–Al layer: 100 µm. Zn–Al plus epoxy system: 425 µm total.	Separate metallic sacrificial inventory from polymer barrier thickness.
Arc-sprayed metallic coatings [9]	Coating: approximately 300 µm. Steel Ra: 3.5 ± 0.5 µm; finished coating Ra: 15–25 µm.	Substrate profile and final outer texture are distinct. Test defects exposed 5% of the surface area.
Microstructured and active surfaces [31,40]	PDMS microtopography with 2 µm feature spacing [40]; nanoscale inhibitor containers [31]. Total film thickness is a separate descriptor.	Report feature dimensions and distribution, damage size, and film thickness; the functional feature size is not the coating thickness.

3.5. Comparative Evidence and Engineering Maturity

Table 3 separates reported performance from the conclusions it can support for ORE selection. Adhesion retention is the post-exposure pull-off strength divided by the initial value under comparable conditioning; fracture mode must accompany the ratio. Electrochemical comparisons require the exposed area, frequency or fitted circuit, electrolyte, temperature, and exposure time. Wear comparisons require matched loading and area. None of these metrics alone defines a maintenance interval: a service-life comparison also

needs a common failure criterion and either its observed crossing time or a censored record showing that failure has not yet occurred.

Table 3. Selected quantitative and comparative evidence, with limits on offshore interpretation. Durations are test or exposure periods, not guaranteed service lives.

System and Evidence	Conditions and Scale	Reported Result	Engineering Interpretation
Zn–Al/epoxy and epoxy [4]	Daebu Island, Korea; 365-day tidal exposure. Nominal total thickness: 425 μm duplex and 500 μm epoxy.	Final pull-off strengths 11.1 and 9.3 MPa, respectively; both decreased by about 29%.	Useful wet-exposure comparison; architecture and thickness differ, so this is not an isolated chemistry effect.
Thermal-spray alloys [9]	Approximately 300 μm; 5% artificial exposed area; 90-day laboratory and six-month marine exposure.	Al-based coatings favored immersion; Zn–15Al was advantageous in atmospheric/splash exposure.	A zone-dependent ranking, not evidence of a universal best metal or long-term depletion rate.
Damaged TSA [34]	1050 Al on steel; approximately 5%–18% holidays; synthetic seawater, 25 °C; 420 days.	Steel potential below −800 mV vs. Ag/AgCl at all tested damage levels; no significant overall performance penalty from damage over the test.	Laboratory sacrificial protection persists at defects; site-specific consumption and defect limits remain necessary.
Four repair coatings [41]	Rotating-wire-blasted steel; Helgoland splash zone, North Sea; 57 months.	Laboratory/field acceleration factors ranged from 5.2 to 8.6; delamination and pull-off responses depended on system and aging.	Field-supported repair assessment; those factors cannot be converted into a universal inspection or repair interval.
Four compressed multilayer systems [21]	Prior compression followed by ISO 12944-9 cyclic exposure.	Coating type and total dry-film thickness explained 86% of analyzed effects; load factors 5%; plastic deformation did not reduce protection.	Mechanical damage is not automatically detrimental; crack formation and interface failure must be demonstrated.
Modified silica/waterborne epoxy [29]	800 ± 50 nm filler; formulation series; 16 AC–DC–AC accelerated cycles.	3 wt.% gave the best corrosion response among the tested loadings.	An optimum within one formulation and test, not a universal nanoparticle loading or validated offshore life.
PDMS-based polyurethane [36]	12.5 wt.% hydroxypropyl-PDMS formulation; 80 h laboratory cavitation.	Cumulative mass loss 2.96 mg; increasing PDMS improved cavitation resistance but reduced adhesion.	Do not compare the mass loss with other rigs without exposed area/loading; qualify the adhesion–wear trade-off in seawater.
Silicone foul-release vs. copper coatings [26]	One silicone- and two copper-containing products; three Baltic sites; one year on static panels.	The silicone product performed as well as or better than the copper systems under the tested conditions.	Direct static-panel evidence; not a universal antifouling ranking, deep-water validation, or complete environmental assessment.
Hydrogen-bonded polyurethane [30]	48 h healing at room temperature; tensile recovery metric.	85% tensile-strength recovery reported.	Mechanical healing is not equivalent to recovery of an immersed corrosion barrier or repeatable offshore self-repair.

Engineering maturity is specific to the substrate, exposure zone, surface preparation, applicator, and complete coating system; assigning all epoxies or all smart coatings one numerical technology-readiness level would conceal these differences. For atmospheric steel, prioritize weathering resistance; for splash/tidal steel, wet adhesion and slow defect growth; for immersed steel, barrier/cathodic compatibility; and for blades or wear regions, wet fatigue and erosion resistance.

Several conclusions converge: preparation and complete architecture matter, isolated initial properties do not predict offshore life, and laboratory acceleration depends on failure mechanism. Important conditional findings also remain: compression need not impair protection [21]; static foul-release performance can be favorable [26]; and an improved wear response can coincide with weaker adhesion [36]. The unresolved comparison is long-term performance of advanced formulations against qualified reference systems at matched thickness, cure, defect geometry, and coupled loading. Comparable wet EIS trajectories, fracture-resolved adhesion, wear loss, ecological release, and repair records are especially scarce in one common experiment. Until that evidence exists, numerical lifetime or maintenance rankings across technology classes would exceed the available support.

Evidence classification. The comparative assessment supports three practical categories for the systems considered here; these are evidence categories, not universal rankings of coating chemistry:

(i) Supported by offshore field evidence: conventional organic multilayers, metallic–organic duplex systems, and selected organic repair coatings have offshore exposure records, including three-year North Sea trials and 57-month splash-zone repair exposures [20,41,42]. Selected thermally sprayed metallic systems also have marine field comparisons [9]. These records support use as reference technologies within the tested conditions, not a guaranteed service life at another site.

(ii) Supported mainly by laboratory studies: the selected nanofiller-modified barriers, ceramic-rich or oxide-modified wear layers, and compliant cavitation-resistant coatings demonstrate formulation-specific benefits under controlled tests [16,27,29,35,36]. Their performance relative to qualified offshore systems still requires matched field comparisons. Silicone foul-release coatings have coastal static-panel and boat-hull evidence [25,26], which should be identified separately from validation on offshore renewable-energy components.

(iii) Emerging technologies requiring offshore field validation: autonomous or stimulus-assisted healing, inhibitor-delivery nanocontainers, corrosion/damage sensing, and integrated responsive multifunctional systems remain proof-of-function approaches in the cited studies [28,30–32,37–39]. Deployment claims require evidence of repeatable function after wet aging and damage, practical application and triggering, and retained protection during representative offshore exposure. This category distinguishes unvalidated active functions from the laboratory material-performance improvements in category (ii); one coating can incorporate both.

4. Coating–Substrate Interaction and Performance

Offshore durability depends on the coating–substrate interface as well as the coating material. Surface condition, adhesion, thickness, defects, and strain compatibility determine whether the system remains protective during exposure. Local failure is particularly consequential where seawater reaches steel that is difficult to inspect or repair.

4.1. Surface Preparation and Adhesion

An appropriate steel surface is clean, dry, wettable by the selected coating, and textured sufficiently for interfacial anchorage without leaving inadequately covered peaks. Visible oil, grease, mill scale, rust, dust, and loose abrasive should be removed; soluble salts require separate assessment because visual cleanliness does not establish chemical cleanliness. Residual salts can create an osmotic driving force after wetting, while oils and weakly attached corrosion products obstruct intimate contact and introduce weak interfacial regions. For blast-cleaned steel, Sa 2½ is a visual preparation grade under ISO 8501-1 [43]; it is not a numerical roughness value. This preparation was used in the offshore-

coating experiments of Eom et al. and Pélissier et al. [4,44]. The allowable salt loading, flash-rust condition, humidity, and substrate temperature relative to the dew point must follow the qualified coating specification; a single acceptance limit should not be imposed on all formulations.

Surface profile must be specified independently of cleanliness. Ra is the arithmetic mean profile-height deviation; a peak-to-valley measure such as Rz, an areal parameter such as Sa, and an ISO 8503-1 grit/shot comparator grade describe different properties and are not interchangeable [45]. The measurement method, filtering/cut-off, sampling length or area, and number of locations should accompany reported values. Pélissier et al. used a medium grit profile, designated MG, whereas Grinon-Echaniz et al. measured Ra = 3.5 ± 0.5 µm on grit-blasted steel and Ra = 15–25 µm on the resulting approximately 300 µm thermal-spray coatings [9,44]. These are experimentally reported values for those processing routes, not universal optimum roughness targets. In particular, a reported Ra cannot be substituted directly for a specified peak-to-valley blast-profile range.

The desirable anchor profile depends on coating rheology and thickness. A distributed angular texture can increase contact area and mechanical interlocking, provided that liquid coating wets the valleys and covers the peaks. Deep isolated pits, embedded particles, sharp asperities, and connected grooves can instead retain contaminants, trap air, concentrate strain, or leave locally thin cover. Therefore, increasing roughness alone does not necessarily improve corrosion resistance. A profile acceptable beneath a several-hundred-micrometre high-build epoxy or thermal-spray layer may be unsuitable beneath a thin hybrid film. Substrate profile, local minimum dry-film thickness, and cross-sectional coverage should be assessed together, especially at welds and edges; an average thickness reading does not exclude exposed or poorly covered peaks [4,9,10,46].

Preparation and deposition must consequently be qualified as a pair. Abrasive blasting generates a fresh anchor profile, while power-tool cleaning produces a different distribution of grooves and residual surface material; water-jet cleaning can remove contaminants but does not necessarily recreate the profile produced by abrasive impact. Surface-tolerant repair epoxies should be evaluated on the actual repair preparation rather than assigned performance from freshly blasted steel [41,46]. Airless spraying of high-build paints requires adequate wetting, stripe coating at edges and welds, control of sagging and entrained air, and compliance with cure and recoat windows. Thermal spraying relies strongly on anchorage of deposited splats, whereas a thin sol–gel layer requires a surface compatible with its limited capacity to cover topography. Hot-dip galvanizing develops a metallurgical coating through chemical pretreatment and immersion, so its preparation criteria differ from those of mechanically anchored sprayed layers [9,10,33].

Adhesion should be measured both before exposure and after wet aging, with the fracture location reported. Failure within the dolly adhesive, between coating layers, within the coating, or at the steel interface has a different interpretation; a numerical pull-off value alone cannot identify loss of coating–steel adhesion. Eom et al. explicitly considered fracture type when assessing marine-exposed systems, and Momber et al. assessed adhesion after three years offshore [4,42]. Record dolly size, loading method, conditioning, scoring, and the fractions of the fracture surfaces associated with each layer, because these variables affect comparability [47].

The finished outer surface serves a different function from the buried anchor profile. Spray texture, pores, exposed fillers, orange peel, and repair steps can increase roughness, while flow and fouling respond to feature height, spacing, and shape. The measured Ra increase from 3.5 ± 0.5 µm for prepared steel to 15–25 µm after thermal spraying demonstrates that deposition creates its own topography [9]. Smoothing or sealing may reduce exposed pathways and facilitate cleaning, but engineered microtextures

can have organism-specific settlement effects [40]. Therefore, a surface rough enough to anchor the coating is not automatically a desirable final hydrodynamic or foul-release surface. Characterize both interfaces and assess changes after immersion, wear, and cleaning [9,25,40].

4.2. Barrier, Mechanical, and Interfacial Performance

An organic barrier restricts transport of water, oxygen, and aggressive ions toward the substrate. Effective protection requires suitable permeability, thickness, cure, interlayer compatibility, and defect control. EIS can detect changes associated with wetting and barrier deterioration, but its interpretation depends on measurement geometry and the physical validity of the fitted model [48].

Barrier performance is closely linked to mechanical integrity. Offshore coatings experience handling damage during fabrication and installation as well as impact, abrasion, cyclic deformation, wave loading, and operational stresses during service. Once cracking, scratching, or delamination occurs, the barrier function becomes locally compromised and seawater can reach the metallic substrate. Three-year North Sea exposure experiments demonstrated that mechanical coating damage can initiate paint delamination and steel corrosion, highlighting the strong relationship between physical integrity and electrochemical protection [20].

This interaction becomes more important when structural deformation is repeated. Organic coatings must accommodate substrate strain without developing cracks or losing adhesion. However, Momber et al. found that coating system and total dry-film thickness dominated corrosion-protection outcomes after compression; plastically deformed regions did not show reduced protection in their test [21]. By contrast, Zhang et al. reported degradation of an epoxy zinc-rich coating/steel system under stress-corrosion conditions [22]. These results address different load histories and failure modes. They support testing wet cyclic strain, crack density, and interfacial failure explicitly rather than assuming a universal penalty from deformation.

For metallic and thermally sprayed coatings, protection is governed by both barrier and electrochemical mechanisms. Aluminum- and zinc-based thermal-spray coatings provide a physical barrier when intact while offering sacrificial protection when steel is locally exposed. However, their effectiveness varies with marine exposure condition. Laboratory and field investigations have shown that aluminum alloys can perform particularly well under full immersion, whereas zinc-containing coatings may offer favorable protection in atmospheric and splash environments [9].

These observations demonstrate that coating performance cannot be adequately represented by a single parameter such as adhesion strength, hardness, or corrosion potential. Offshore qualification should instead consider the combined evolution of barrier resistance, adhesion, mechanical damage tolerance, and interfacial corrosion.

Length-scale reasoning helps interpret these measurements. In an ideal, homogeneous, defect-free film governed by one-dimensional Fickian diffusion, the characteristic transport time scales with thickness squared divided by effective diffusivity. Doubling thickness would therefore increase this characteristic time fourfold only if diffusivity and boundary conditions were unchanged; this is a model scaling, not a fourfold service-life prediction. A through-thickness pore or interfacial path can bypass that benefit. Coating capacitance likewise depends on dielectric response, area, and thickness, so water uptake cannot be inferred from an impedance change without considering swelling, ionic conduction, and model validity [48]. Mechanical comparisons should additionally report wet modulus, strain to failure, glass-transition behavior, and interfacial fracture mode; a stiff, thick layer

can store more elastic energy available to drive delamination even when its initial adhesion is high [21,22].

A useful EIS comparison follows the evolving coating resistance, coating capacitance or appropriately interpreted constant-phase element, and interfacial charge-transfer response, while checking that the equivalent circuit remains identifiable. Bongiorno et al. compared coatings of different pigment volume concentration on AA2024-T3 and mild steel in four electrolytes; a corrosion-charge estimate from time-resolved EIS correlated with substrate corrosion assessed after removing the coating [49]. Thus, a time series linked to an independent substrate endpoint can be more informative than one low-frequency impedance value. This does not supply a universal impedance threshold, and an absolute capacitance or resistance ranking is invalid when exposed area, thickness, hydration, or circuit assignment differs. Report uncertainty and retain the raw spectra alongside fitted parameters.

4.3. Durability and Environmental Compatibility

Durability is ultimately determined by the ability of a coating system to preserve its protective functions over the intended service period. Long-term field exposure is particularly valuable because degradation under real offshore conditions includes interactions among seawater, temperature, biofouling, mechanical damage, and exposure-zone effects that are difficult to reproduce simultaneously in the laboratory. For example, repair coatings exposed for 57 months in the North Sea splash zone exhibited coating-dependent changes in delamination and pull-off strength, while comparison with accelerated laboratory testing produced acceleration factors that varied substantially among systems [41].

Such results reinforce the importance of designing coating systems for the actual component and exposure environment rather than relying exclusively on standardized laboratory performance. For difficult-to-access ORE structures, extending coating durability can provide additional benefits by reducing offshore inspection, repair, vessel operation, downtime, and associated lifecycle costs.

Environmental compatibility should simultaneously be considered. Coating manufacture, application, maintenance, degradation, and removal can contribute to environmental impacts through energy and material consumption, solvent emissions, release of coating constituents, and waste generation. Lifecycle assessment of offshore wind-turbine coating systems has demonstrated that coating formulation and protection strategy can significantly influence overall environmental performance and provides a quantitative basis for comparing more sustainable alternatives [50].

Consequently, future coating design should balance high adhesion, barrier efficiency, mechanical durability, repairability, environmental compatibility, and service life. A coating with excellent initial corrosion resistance may not represent the optimal offshore solution if it exhibits poor damage tolerance, requires frequent maintenance, or generates substantial environmental burdens.

Environmental comparisons also require explicit scales and exposure conditions. Report released mass per coated area and time, distinguish dissolved from particulate material, and document water chemistry, renewal rate, abrasion, and cleaning. A low release rate in static immersion cannot establish the same behavior under erosive flow. Coating lifetime and material consumption should be evaluated over the same protected area and service duration; otherwise a thin coating with frequent replacement can appear preferable to a thicker, longer-lived system solely because the accounting boundary excludes maintenance [6,50,51].

Environmental preference should also be supported at the product and exposure level. The Baltic comparison [26] supports silicone foul-release as a practical alternative

to copper-containing antifouling products under the tested conditions, but the study also discusses limitations in the environmental evidence for silicone systems. Absence of a declared biocide does not establish harmless leachate, and lower VOC during application does not establish lower marine toxicity. Compare release under immersion and cleaning, effects on relevant non-target organisms, coating removal waste, and replacement frequency over a common protected area and time. A waterborne formulation or an active nanocontainer should not be labeled eco-friendly solely from solvent content or targeted release behavior [6,26,29,50].

5. Testing and Performance Assessment

Offshore qualification requires evidence that a coating resists the chemical, biological, and mechanical stresses relevant to its duty. Accelerated tests provide reproducible comparisons, but acceleration may change the dominant mechanism and does not imply a universal conversion to service years [7,10,15,20,41,44]. A defensible assessment combines material characterization, controlled aging, matched field exposure, and component-specific multi-stressor tests.

The methods in Sections 5.1 and 5.2 measure complementary responses: corrosion exposure establishes boundary conditions, electrochemistry probes barrier and interface behavior, mechanical tests assess attachment and deformation, and microscopy locates damage. Figure 3 integrates those measurements into a controlled comparison and a field-validation gate. It is an experimental-design schematic, not an equipment photograph or a report of new instrument data [4,9,10,44].

5.1. Laboratory and Accelerated Testing

Laboratory characterization generally includes coating thickness, adhesion, hardness, impact and abrasion resistance, water uptake, and electrochemical properties. Pull-off testing is widely employed to assess coating–substrate adhesion, whereas EIS provides a sensitive, non-destructive method for monitoring changes in barrier properties during electrolyte exposure [4,47,48]. Microscopy and surface characterization can further identify blistering, cracking, delamination, corrosion products, and other damage that may not be adequately represented by a single quantitative parameter.

Accelerated aging typically employs neutral salt spray, seawater immersion, humidity, UV/condensation cycling, temperature cycling, and cathodic-disbondment testing [7,10,15,44]. For offshore carbon-steel structures within its scope, ISO 12944-9 provides one of the principal qualification frameworks for protective paint systems exposed to offshore atmospheric CX and seawater-immersion Im4 environments with cathodic protection [7]. Its cyclic-aging approach represents an improvement over continuous salt-spray exposure by sequentially introducing UV/condensation, chloride exposure, and low-temperature conditions.

A salt-fog chamber supplies and distributes aerosol over supported test panels, whereas cyclic aging additionally changes moisture, UV, and temperature conditions. ASTM B117 specifies operation of a salt-fog apparatus; it does not by itself provide a universal coating pass criterion or conversion to offshore years [52]. The cyclic procedure used by Pélissier et al. comprised 72 h of UV/condensation, 72 h of neutral salt spray, and 24 h at −20 °C, repeated to 4200 h [44]. This requires the appropriate exposure stages with suitable apparatus for each stressor. Record scribe geometry, edge sealing, replicates, and ratings of rusting, blistering, and scribe creep because they govern what is being compared [10,44].

An EIS setup comprises a potentiostat/frequency-response system, an electrochemical cell, and data display. The coated specimen is the working electrode; the reference electrode provides a stable potential, and the counter electrode completes the current path. A small

alternating perturbation is applied over a frequency range. Nyquist plots relate the real and imaginary impedance components, whereas Bode plots show magnitude and phase against frequency. Coating resistance/capacitance describe barrier response; a newly resolved interfacial time constant may indicate electrolyte access to the substrate. Interpretation should report exposed area, electrolyte, temperature, perturbation amplitude, frequency range, and equivalent-circuit uncertainty. A high impedance magnitude alone is not a universal lifetime guarantee, and a semicircle is not automatically evidence for one unique process [48].

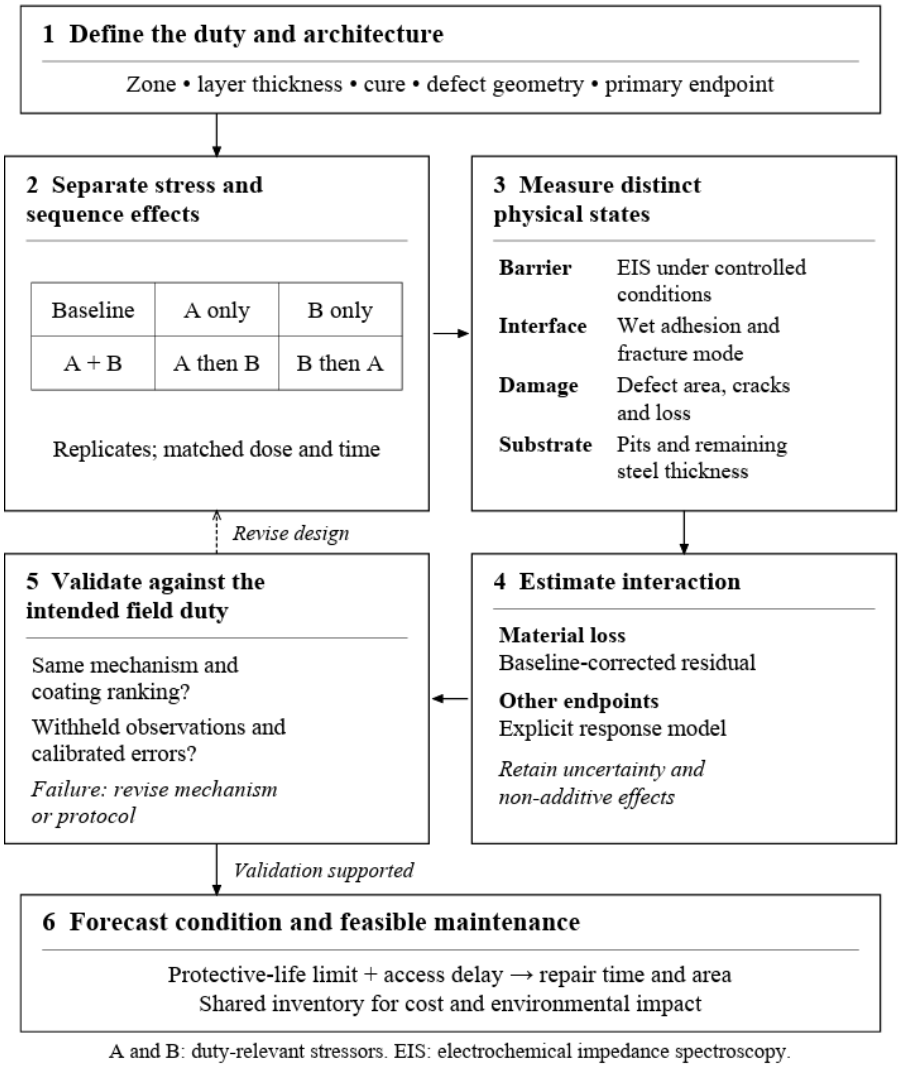


Figure 3. Proposed workflow for multi-stressor qualification and lifecycle transfer. A and B are two duty-relevant stressors; the baseline, isolated, simultaneous, and sequential groups use comparable conditioning and independent specimens. The workflow links distinct physical endpoints to interaction estimates and field validation before prognosis.

Polarization testing uses a potentiostat and electrode cell to vary potential and record current. Anodic and cathodic branches can provide corrosion potential and, where the kinetic assumptions are satisfied, estimates of corrosion current. For intact resistive paints, mixed exposed/coated areas, diffusion control, or sacrificial metallic layers, simple Tafel extrapolation can be misleading. The measured area and current-carrying surface must be identified, and large polarization excursions can alter the specimen. Consequently, corrosion-rate estimation is conditional: it does not establish the corrosion rate beneath every intact coating or predict an offshore lifetime [9].

Pull-off testing uses a loading device acting on a dolly bonded to the coating. The reported stress is the applied tensile force divided by dolly area, with fracture location and test conditions recorded. Taber abrasion uses a rotating coated specimen contacted by loaded abrasive wheels. Report wheel type, applied load, cycles, conditioning, and mass or thickness loss. Taber abrasion measures a defined contact-wear response and should not be treated as a direct simulation of sediment impact, cavitation, or all marine erosion modes [4,47,53].

Pencil hardness ranks film hardness through pencil-induced damage (ASTM D3363), whereas Shore indentation probes a different response (ASTM D2240) and requires a suitable material and specimen thickness/support [54,55]. They are not interchangeable scales. The impact test uses a falling mass and indenter to impose rapid deformation on a coated panel; drop conditions and substrate geometry govern the resulting cracking (ASTM D2794) [56]. The mandrel-bend test imposes curvature, and resistance to cracking depends on substrate geometry as well as coating flexibility (ASTM D522/D522M) [57]. These loading modes require the corresponding specimen geometry, apparatus, and evaluation procedure [54–57].

Cathodic-disbondment testing uses an electrolyte bath with a deliberately damaged coated specimen polarized relative to a reference electrode. It measures lateral adhesion loss around the holiday under specified potential, temperature, electrolyte, and time; negative potential should not be reported without naming the reference electrode [23]. Gravimetric water uptake is measured with a balance and requires a dry baseline, controlled immersion and surface-water removal, and repeated mass measurements. ASTM D570 provides a water-absorption method for suitable plastic specimens; specimen geometry and the presence of a steel backing must be considered when designing a coating-specific measurement [58]. One balance reading does not determine permeability. Separate permeation measurements or a justified transport model are required, and dissolution or leaching can confound mass gain [48,58].

SEM/EDS analysis combines an electron microscope, specimen stage, electron detector, and X-ray analysis. SEM resolves morphology, pores, cracks, and polished cross-sections; EDS maps or estimates elemental composition. These measurements help locate interfaces and corrosion products, but EDS alone does not establish oxidation state, biological identity, or MIC. Quantitative images should include scale bars and sampling locations. Cross-sectional thickness, pore connectivity, and local damage should be compared with the area-averaged electrochemical and mechanical measurements. These methods provide local structural and compositional evidence [9].

Accelerated testing can effectively differentiate coating formulations and identify early failure mechanisms. Evaluation of 12 coating systems for offshore wind monopiles, for example, demonstrated clear differences among systems intended for atmospheric, splash, and submerged zones [10]. However, the coatings did not exhibit equivalent acceleration rates, and some laboratory immersion results were substantially less severe than corresponding offshore exposure. Similarly, long-term comparison of 11 marine coating systems showed that correlations between accelerated and field tests depended on both the selected accelerated protocol and the exposure site [44].

Consequently, an accelerated test should not automatically be interpreted through a universal laboratory-to-service-life conversion factor. Test severity must be sufficient to accelerate relevant degradation without introducing unrealistic failure mechanisms. Recent reviews of marine coating aging similarly emphasize the importance of linking artificial aging conditions with the actual environmental factors and degradation mechanisms expected during service [15].

5.2. Field Exposure and Offshore Validation

Field exposure remains essential for validating coating performance because specimens are subjected to natural variations in salinity, temperature, solar radiation, wetting–drying cycles, waves, marine aerosols, biological activity, and mechanical damage. Long-term offshore investigations have demonstrated that coating degradation varies substantially with exposure zone and coating architecture [10,20,41,42].

Three-year offshore exposure studies showed that organic and duplex coating systems differed considerably in adhesion retention and damage propagation [20,42]. Longer-term splash-zone exposure further demonstrated coating-dependent changes in delamination and pull-off strength, emphasizing that laboratory acceleration factors are not necessarily transferable among different coating systems [41]. Such observations are particularly relevant to ORE structures, where a single foundation may simultaneously include atmospheric, splash, tidal, and permanently submerged regions.

Direct laboratory–field comparisons provide additional evidence of this limitation. Marinova et al. [10] found significant discrepancies between laboratory seawater immersion and offshore exposure for some monopile coatings. Pélissier et al. [44] similarly compared organic coating systems exposed at a stationary marine site and on an operating vessel with ISO 12944-9 and a modified protocol based on ASTM D5894 [59]. The correlations depended strongly on both the exposure environment and accelerated method, demonstrating that a coating ranking obtained using one laboratory protocol may not necessarily remain unchanged under actual marine conditions.

The disagreement is informative rather than a reason to abandon accelerated testing. For the 11 systems assessed by Pélissier et al., correlations depended on exposure duration and the systems included in the regression; satisfactory agreement for the modified ASTM D5894 protocol at the stationary site required excluding the epoxy glass-flake system S8 and at least seven years of exposure [44]. In the Helgoland repair-coating study, acceleration factors of 5.2–8.6 depended on the coating and response considered [41]. A qualifying test should consequently reproduce the intended failure mode and preserve relative ranking for the target zone. Neither a standard's nominal duration nor a factor borrowed from another formulation establishes the date when an ORE asset will need repair.

Field validation should reproduce the same coating batch, measured thickness, preparation grade, and defined defect geometry used in laboratory comparisons. Deploy paired intact and scribed specimens in the relevant atmospheric, splash/tidal, and immersed positions, with the submerged cathodic-protection condition recorded. Document temperature, salinity, oxygen, wetness, flow, seasonal fouling, cleaning, and handling damage. The proposed comparison is between time histories of scribe creep, rusted area, wet adhesion, and impedance (where feasible), followed by cross-sectional examination. The first validation criterion is agreement in failure location and mechanism; only then should coating ranking or an acceleration factor be transferred. Stationary racks do not validate a rotating blade or a strained cable coating without additional representative loading [10,20,41,44].

Field exposure studies use coated panels at defined marine exposure positions to compare coating performance [4,9,10,44]. Corrosion-monitoring and prognosis approaches provide a basis for selecting measurement channels [8], while EIS can characterize coating barrier response under controlled measurement conditions [48]. An asset-specific monitoring arrangement may combine an immersed probe, a surface-connected sensor, and a data logger/telemetry unit for local measurement and time-stamped recording or transmission. Report sensor principle, location, calibration, reference-electrode stability, power/data availability, and cleaning history. A buoy or logger does not directly measure adhesion or every coating property. Pair repeated local measurements with retrieval, photography, and thickness measurements; assess pull-off adhesion separately on matched specimens using

the applicable procedure [47]. Recognize that a sensor samples only a small region of a large asset.

5.3. Multi-Stressor Testing

A major remaining challenge is the development of tests capable of reproducing coupled offshore degradation. Conventional methods generally focus on environmental aging, whereas ORE coatings can simultaneously experience corrosion, UV radiation, thermal cycling, cyclic strain, impact, abrasion, erosion, cavitation, and biofouling. Damage produced by one mechanism may substantially alter susceptibility to another.

Mechanical damage is particularly important. Impact, compression, abrasion, or fatigue-induced cracking can locally compromise the coating barrier and expose the steel substrate to seawater. Conversely, electrolyte penetration and underfilm corrosion may weaken coating adhesion and increase susceptibility to mechanical delamination [20–22]. This bidirectional interaction means that testing a pristine coating under corrosion exposure alone may overestimate its protection under actual operating conditions.

Corrosion–fatigue illustrates the broader importance of environmental–mechanical coupling. Offshore wind foundations are subjected to persistent cyclic wind and wave loading in corrosive environments. Mehmanparast and Vidament [60] proposed temperature-based acceleration equations for seawater S–N and crack-growth testing and validated their predictions against existing fatigue data. Although such testing primarily addresses structural steel, the same principle is important for coating qualification: environmental exposure and cyclic loading should increasingly be assessed as interacting processes rather than independent tests.

Table 4 proposes four component-specific combination schemes. These are research protocols to be calibrated against site histories, not newly established qualification standards. Simultaneous exposure is used when the stresses interact during operation; sequential exposure is used to test aging memory or a change of environment. A submerged surface should not receive an arbitrary UV dose, and a laboratory strain frequency should not be increased so far that heating or loss of electrochemical equilibration changes the mechanism.

Table 4. Proposed component-specific multi-stressor schemes, controls, and mechanism-discriminating measurements.

Component and Mechanism	Proposed Stressor Combination and Sequence	Controls and Distinguishing Measurements
Atmospheric/upper splash steel UV aging → strain-assisted ingress	Use the published 168 h block: 72 h UV/condensation, 72 h salt spray, then 24 h at −20 °C, repeated to the specified endpoint [44]. In a separate modified arm, add calibrated cyclic substrate strain during the wet stage. Compare pre-aged-then-loaded with loaded-then-aged specimens at matched doses.	Retain the unmodified cyclic exposure and strain-only controls. Match temperature and elapsed time. Measure cracking, wet adhesion, scribe creep, and EIS. The added-strain arm is a research modification, not ISO 12944-9 compliance.
Splash/tidal foundation Wet–dry cycling + impact + strain	Repeat saline wetting and drying using the site immersion duty cycle. Apply substrate strain during wetting and calibrated impact or abrasion at stated block boundaries. For a tidal region with cathodic protection, polarize only during the wetted stage and record potential versus the reference electrode [10,20–22].	Include wet–dry only, load only, pre-damaged exposure, and reverse-order groups. Record local strain, salt accumulation, hydration, impact dose, defect growth, wet adhesion, and substrate attack.

Table 4. *Cont.*

Component and Mechanism	Proposed Stressor Combination and Sequence	Controls and Distinguishing Measurements
Submerged steel/moving connections Cathodic disbondment + biofilm + cyclic strain	Continuously immerse in oxygen- and flow-controlled seawater; compare site-representative cathodic protection with unpolarized specimens. Superimpose the measured strain spectrum. In a separate biological branch, establish fouling before loading and compare with an otherwise matched abiotic control [3,8,23].	Start with pairwise comparisons, then selected full combinations. Control changes introduced by sterilization. Measure disbonded area, potential/current, biofilm coverage, local chemistry, wet adhesion, and metal loss; record specimen temperature.
Tidal rotor/wear-exposed part Erosion–corrosion; cavitation where relevant	Combine flowing seawater with calibrated particle size, concentration, velocity, and impact angle. Add cavitation in a separate arm only when representative pressure conditions justify it. Compare simultaneous wear–corrosion with wear followed by immersion and immersion followed by wear [14,16,24].	Use corrosion-only and mechanically dominated controls; identify effects of corrosion suppression on the surface. Measure volume/thickness loss, current (where interpretable), crack morphology, and interfacial failure. Do not pool polymer and substrate mass losses.

For every scheme, use a reference coating and candidate system at matched measured thickness and cure; include intact and identically damaged variants. For two stressors, include baseline, A-only, B-only, A-with-B, A-then-B, and B-then-A groups, matching cumulative dose and elapsed conditioning time as closely as the physical comparison permits. A practical starting design uses at least three independent specimens per condition, with replicate number then justified by pilot variability and statistical power; repeated readings of one panel are not independent replicates. Prespecify temperature, electrolyte renewal, oxygen, flow, exposure duration, stress amplitude, and the primary endpoint. Report whether any mismatch in dose, rest time, or hydration could explain an apparent interaction.

The shared endpoints should include delamination distance, rusted-area fraction, crack density, remaining thickness, and wet adhesion with fracture mode. Record EIS at comparable temperature and hydration on suitable specimens, and use sacrificial replicates for destructive pull-off and cross-sectional analyses. For wear–corrosion, compare total loss with mechanically dominated and corrosion-only controls and apply the material-loss accounting described in Section 2.4 [16,24]. For biological coupling, record coverage, species/community information, oxygen and pH alongside corrosion; fouling alone does not establish MIC. Validate both failure mechanism and ranking against Section 5.2 field exposures before converting a laboratory trajectory into a lifetime prediction [10,21,22,41,44,60].

A candidate should advance to offshore validation when its limiting failure mode is understood, its repeatability is documented, and its benefit exceeds measurement and specimen variability. Figure 3 shows this sequence. The matched groups separate simultaneous interaction from exposure-order effects, while the measurement channels retain the distinction between coating damage and substrate loss.

6. Service-Life and Lifecycle Design

Coating selection should account for the full protection period, including inspection and the time needed to reach damaged regions. Weather windows, vessel availability, safety requirements, and downtime can make offshore repair substantially more demanding than fabrication-stage application [8,61]. Condition assessment, remaining-life prediction,

maintenance planning, cost, and environmental inventories should therefore use a common degradation history.

6.1. Inspection and Service-Life Prediction

Inspection provides the essential link between coating degradation and structural integrity management. Conventional offshore inspection includes visual assessment, coating-thickness measurement, adhesion testing, ultrasonic thickness measurement, and other non-destructive testing (NDT) techniques. Visual inspection remains important for identifying rusting, blistering, cracking, and delamination; however, deterioration beneath apparently intact coatings may remain undetected during its early stages. Remote and continuous monitoring techniques are therefore receiving increasing attention for offshore structures, particularly where physical access is difficult or hazardous [8].

Inspection requirements should be tailored to the exposure environment and consequence of failure. Splash and tidal zones generally require particular attention because cyclic wetting and drying, chloride accumulation, oxygen availability, wave action, and mechanical damage can accelerate coating deterioration and substrate corrosion [1]. Permanently submerged components, in contrast, require consideration of coating integrity together with cathodic protection, biofouling, and microbiologically influenced corrosion. Inspection intervals should therefore not be determined solely by coating age but should incorporate environmental severity, coating architecture, application quality, observed damage, accessibility, structural criticality, and previous maintenance history.

Coating prognostics require location-specific degradation records. For each mapped surface region, retain initial layer thickness and preparation/cure records, then time series of defect area, delamination distance, rusting, local electrochemical response, and steel thickness or pit depth. Record wet adhesion on matched witness panels or sampled areas because pull-off testing itself damages the coating. Brijder et al. describe corrosion monitoring and probabilistic prognostics for offshore structures; adapting that framework to a coating requires a separate observation model for each measurement [8]. Area-normalized impedance is a barrier indicator under stated test conditions, whereas ultrasonic thickness measures substrate loss; neither can substitute directly for the other.

A practical model separates an intact or wetted barrier state, an actively corroding defect state, and a spreading delamination state. Fit transition rates or continuous damage-growth parameters to repeated field observations, with dependence on exposure zone, temperature, mechanical loading, and cathodic protection where data permit. For example, the long-term repair-coating study reporting delamination and pull-off performance after 57 months provides relevant validation endpoints, while the three-year offshore adhesion study tests retention of interfacial function [41,42]. A single endpoint is not enough to identify a full growth law: intermediate inspections, uncertainty, and specimens that have not failed must be retained. Separate random variability between locations from uncertainty caused by sparse data.

Define remaining protective life as the distribution of time until an agreed coating criterion is first crossed, conditional on the measurements to date. Possible criteria include excessive defect growth or loss of wet adhesion, with a separate limit for structural metal loss. Impedance thresholds must be calibrated for the specific coating and measurement configuration; one universal impedance value is inappropriate. Generate predicted trajectories using the fitted parameter uncertainty, update them as inspections arrive, and report the probability of crossing the criterion before the next feasible intervention. Validate on a withheld period, coating batch, or site, and assess both prediction error and uncertainty coverage. A digital twin should not report a precise coating lifetime from an unvalidated structural-fatigue model [8,41,42,62].

The data-to-decision record has four linked elements: defect mapping and wet adhesion constrain damage growth; barrier measurements constrain electrolyte access; direct steel measurements constrain substrate loss; and predicted repair dates and areas determine intervention inventories. Each observation retains its own spatial resolution and uncertainty. This common record prevents RUL, LCC, and LCA from relying on incompatible service-life assumptions.

6.2. Maintenance and Lifecycle Cost

Maintenance represents an important component of offshore wind lifecycle expenditure because offshore interventions require specialized vessels, personnel, equipment, favorable weather windows, and potentially turbine shutdown [61]. Ren et al. [61] emphasized that maintenance strategy, scheduling, onsite operations, accessibility, and environmental conditions are closely interconnected in offshore wind farms. These considerations are equally relevant to coating maintenance because repair frequently requires surface preparation and coating application under substantially less controlled conditions than those available during fabrication.

Underwater maintainability changes the initial design choice. Removing fouling and corrosion products, reaching sheltered interfaces, controlling soluble contamination, and obtaining a suitable surface for bonding are difficult under flow and limited visibility. An underwater-curing repair material must be qualified for the actual substrate condition, temperature, pressure, application method, cure time, and post-cure wet adhesion; dry-shop performance does not establish those properties. Cleaning itself can enlarge a defect or remove a soft functional surface. Repair specifications therefore need acceptance criteria for the prepared area, sound-coating overlap, minimum cover, and verification after cure, alongside the access method. The strong preparation dependence of offshore repair-coating performance reinforces this requirement [41,46].

The practical intervention options differ by component. A local underwater patch may be feasible where a qualified material and remotely operated vehicle or diver can reach the damage; a controlled dry enclosure may be needed where surface preparation or cure cannot be achieved wet; removable modules or selected floating assets may permit retrieval or tow-to-port. Each option introduces distinct access, connection/disconnection, handling, and downtime requirements, and none should be assumed feasible for every foundation [61,63]. Where repair cannot be assured during the service period, this critical narrative review favors greater initial damage tolerance and redundant corrosion control, protected edges and welds, accessible monitoring locations, and replaceable wear-prone parts. Autonomous healing should not be credited as a maintenance strategy until its underwater performance is demonstrated.

Maintenance strategies can broadly be classified as corrective, preventive, and condition-based. Corrective maintenance delays intervention until deterioration becomes significant, potentially reducing short-term expenditure but increasing the probability of extensive underfilm corrosion, substrate loss, and unplanned downtime. Preventive maintenance relies on predetermined inspection or recoating intervals but may result in unnecessary intervention while a coating remains functional. Condition-based maintenance instead uses inspection and monitoring information to determine when intervention is technically and economically justified [8,61,64].

Economic assessment should include preparation, materials, application, quality control, inspection, access, repair, downtime, removal, waste treatment, and decommissioning. A higher initial coating cost may be justified if slower degradation reduces offshore intervention. The comparison remains component-specific because access, recurring damage, and repair effectiveness can outweigh the material price.

The measured degradation trajectory determines the maintenance inventory. Expanding defect and delamination areas estimate the area requiring preparation and recoating, including the overlap needed to reach sound coating. The predicted threshold-crossing time determines the likely campaign date; wet-adhesion and fracture observations determine whether local patching or wider removal is plausible. Steel-thickness or pit-depth observations identify when substrate repair must be added. Expected lifecycle cost is then the initial installed cost plus the probability-weighted, discounted costs of these interventions, access, inspection, downtime, and residual failure consequences over the common analysis horizon. Vessel mobilization is a campaign cost and should not be multiplied independently by every square metre of a shared campaign [41,46,50,61,63,64].

The scheduling decision should compare the probability of reaching the coating or structural limit during the combined procurement and weather-access delay with the consequence of doing so. A coating with slower defect growth can therefore be preferable even when its material cost is higher, because it may allow repair to join a planned vessel campaign. Conversely, an inexpensive surface-tolerant repair may be rational on accessible steel with low failure consequence. Repairs should reset only the treated region in the model, with a repair-effectiveness distribution supported by subsequent inspection; they should not automatically return the whole asset to an as-new state. These are proposed coating-specific extensions of offshore maintenance optimization, not validated cost savings for the systems reviewed here [41,61,63,64].

Cost comparisons should use a common analysis horizon and discount assumptions, include the probability and timing of repair, and distinguish coating work from vessel mobilization and production loss. A condition-based intervention may be economical when it can share vessel access with other work, whereas the same repair may be expensive as a dedicated campaign. Sensitivity to access delay, defect growth, repair effectiveness, and the consequence of missed deterioration should be reported. The optimization output is therefore conditional on logistics and reliability assumptions, not an intrinsic ranking of coating materials [50,61,63,64].

An explicit access-delay allowance is needed between a condition alert and the protective-life limit. Predict defect growth during the waiting period and test a missed-weather-window scenario, rather than scheduling work exactly at the mean predicted failure time. For immersed steel, verify that the cathodic-protection design can accommodate the credible increase in exposed area until repair; protection of steel does not imply that a disbonded coating is restored. Sensitivity cases should include ineffective patching and a larger-than-observed hidden disbonded area. This links poor underwater maintainability directly to the preferred coating architecture and the economic value of reliable condition information.

6.3. Sustainable and Data-Driven Coating Design

Lifecycle design must increasingly incorporate environmental performance alongside durability and cost. Corrosion-protection systems consume raw materials and energy during manufacture and application and may release metals or organic constituents into the marine environment during installation, weathering, abrasion, maintenance, and removal [6]. Environmental compatibility should therefore be considered from coating production through end-of-life rather than being treated solely as a formulation-level requirement.

Lifecycle assessment (LCA) provides a systematic framework for quantifying these impacts. Previous analyses of offshore corrosion-protection systems have demonstrated the value of comparing coating alternatives in terms of material consumption, application, maintenance, and service-life extension [50]. Broader work on marine coatings has

similarly shown that coating selection can influence both environmental and economic performance over an asset's lifecycle [51]. Demirel et al. [51], for example, developed an LCA methodology incorporating coating production and application, fouling-related operational effects, and maintenance requirements, demonstrating the importance of evaluating coating performance at the system level.

For ORE structures, environmental comparison must extend beyond coating manufacture. Greater initial material input may be justified by fewer interventions or avoided steel replacement, but that benefit must be evaluated against production burdens, release, toxicity, and end-of-life treatment. The relevant comparison is protection of the same substrate and area over the same duration and to the same performance criterion.

For LCA, use protection of one square metre of a specified substrate and exposure zone over a stated period to the same performance criterion. Convert each predicted intervention from Section 6.2 into quantities of abrasive, coating, solvent (where relevant), energy, removed material, waste treatment, vessel fuel, and replacement steel. Include application losses and realistic repair overlap. Use measured or justified fouling-related operational effects only where the component response is known; ship-hull fuel penalties cannot be transferred directly to a wind foundation [50,51]. Evaluate impact categories separately and propagate the same lifetime and repair-frequency uncertainty used for LCC. Coating-specific leaching or wear-release measurements inform the emission inventory, but EIS, nominal filler content, or a lower repair frequency does not itself establish low aquatic toxicity [6,50].

A coating digital twin should implement a repeatable data-to-decision sequence: register each measurement to a surface location and time; update the estimated barrier, defect, delamination, and substrate states; forecast their evolution under the expected exposure and access window; and compare feasible inspection or repair actions. The required data include units, inspected area, method, calibration, missing records, and uncertainty, as well as the measured value. A sensor reading from a small accessible region should not be assigned to an unobserved submerged foundation without a justified spatial model [8,62].

The measurement channels constrain different states. Repeated local EIS can inform wetting and barrier deterioration under controlled geometry; image analysis estimates visible defect and fouling coverage; cathodic-protection potential/current records constrain the electrochemical environment; and ultrasonic measurements constrain substrate loss. Wet pull-off and microscopy on witness panels or retrieved samples help interpret changes that an online sensor cannot identify. If these channels disagree, the model should widen uncertainty or trigger a targeted inspection rather than average them into an apparently precise condition score. Temperature, fouling, electrode drift, and changes in measurement area should enter the observation model as potential confounders [8,9,42,48].

The proposed minimum useful digital implementation is a location-indexed condition register linked to a calibrated degradation model and a documented maintenance rule. A more complex machine-learning model is justified only if it improves withheld-data prediction or changes a decision with demonstrable value. Mechanistic constraints can enforce nonnegative loss and plausible transport or damage trends, but an assumed diffusion law cannot describe a newly opened through-thickness crack without a change of model. Remaining-life forecasts must retain alternative failure mechanisms when the data cannot distinguish them.

The structural digital twin demonstrated by Pacheco-Blazquez et al. supplies an example of an updating workflow, not a validated coating-life model [62]. A coating module needs separate calibration before passing corrosion initiation, affected area, or

metal-loss distributions to the structural model. Cost and environmental modules must then use the same forecast repair dates, areas, and materials.

A sustained impedance decline may trigger inspection, while defect growth, loss of wet adhesion, and steel loss update different model states. The maintenance decision then depends on whether a physical limit is likely to be crossed before feasible access. Stable substrate condition may support continued monitoring; accelerating damage may justify earlier repair. Numerical thresholds, observation errors, and intervention performance must be established for the asset before this logic is used operationally.

Taken together, the preferred lifecycle strategy is to invest in reproducible application and a durable primary protection system, then use measured condition to manage the residual uncertainty. Sensor and digital functions are valuable when they alter an inspection or maintenance decision; they cannot compensate for inaccessible repair, poor preparation, or unqualified barrier performance. The following considerations connect data quality, inspection capability, risk, and environmental accounting.

Model inputs should identify environmental and loading histories, the layer stack, and the origin of laboratory, field, and monitoring records. Thickness, porosity, adhesion, permeability, and glass-transition temperature describe different aspects of performance. The evidence synthesized here mainly concerns coated steel and should not be transferred automatically to concrete. Retrieved damage and application records should update subsequent material and process decisions [9,20,41,50].

Inspection can combine continuous local sensing, remote inspection, and close examination. Electrochemical impedance, open-circuit potential (OCP), and linear polarization resistance (LPR) characterize different electrochemical responses; OCP alone is not a corrosion-rate measurement. Remotely operated/autonomous underwater vehicles (ROV/AUV) provide access and imaging, with resolution affected by fouling and water conditions. Ultrasonic testing (UT), acoustic emission (AE), and eddy-current testing (EC) require method-specific calibration and access; they do not all measure coating condition directly. Maintenance choices distinguish time-based prevention, condition-based prediction, and prioritization by probability and consequence of failure [8,9,61,62,64].

Uncertainty in remaining protective life should be reported as a conditional distribution of time to a defined physical endpoint. Transport, electrochemistry, delamination, pit growth, and erosion may require competing models if monitoring does not distinguish the controlling mechanism. A mean forecast and a stated prediction interval can support planning only after calibration; the maintenance date is a decision variable, while failure is defined by a physical condition criterion. None of the cited structural digital-twin workflows establishes a universal coating lifetime [8,41,62].

Risk combines failure probability with the corresponding consequence over a defined period. Candidate maintenance/coating strategies can be compared by cost and risk; a Pareto frontier comprises options for which one objective cannot improve without worsening the other [65]. Selection among those options requires explicit decision preferences and engineering constraints. Sustainability assessment extends the accounting to production, use, access, decommissioning, environmental impacts, worker safety, and recovery. These criteria require compatible system boundaries and should not be collapsed into an unqualified single score. Lifecycle cost and maintenance assumptions should be grounded in offshore O&M evidence [61,63,64], while environmental comparisons require compatible LCA boundaries [50,51]. These sources inform the proposed framework; they do not validate a coating-specific optimum.

6.4. Illustrative Calculation from Condition to Intervention

This worked example makes the connection between coating condition, RUL, LCC, and an LCA inventory explicit. All numerical inputs in Tables 5 and 6 are assumed for demonstration; they are not measurements, supplier quotations, published emission factors, or field-calibrated parameters. The example represents a 1000 m^2 coated-steel region in splash exposure. The decision is made at year 4 and compared over years 4–8. It illustrates a transparent calculation consistent with the monitoring and lifecycle principles above [8,50,61,64], not an optimized coating selection or a prediction for an operating asset.

Table 5. Assumed condition inputs and calculated protective-life outputs. All values are illustrative.

Quantity	Assumed Input or Calculated Result	Interpretation
Coated region and horizon	1000 m^2; decision at year 4; horizon to year 8	Same region and duration for both strategies
Affected area fraction	Year 0: 0.01; year 2: 0.02; year 4: 0.04	Assumed mapped history; no experimental observations
Growth rate k	0.3466 $year^{-1}$	Derived from the assumed history
Protective-function threshold	flim = 0.10	Assumed criterion; separate structural check required
Central RUL at year 4	2.64 years; crossing at year 6.64	No repair and constant local growth rate
Rate sensitivity	k = 0.25–0.45 $year^{-1}$ → RUL = 3.67–2.04 years	Scenario range, not statistical uncertainty bounds
Repair overlap factor	1.25 × affected area	Includes assumed preparation onto sound coating
Access contingency	0.5 years beyond the nominal campaign date	Screen against faster growth before scheduling
Post-repair mapped fraction	f = 0.005 immediately after intervention	Assumed whole-region residual; verify by inspection

Table 6. Assumed intervention inventories and calculated incremental outcomes over years 4–8. Costs are discounted to year 4; climate impacts are not discounted.

Input or Result	Year 5 Shared Campaign	Year 6 Dedicated Campaign
Affected fraction at repair, calculated	0.05657	0.08000
Repair area including overlap, calculated	70.71 m^2	100.00 m^2
Unit repair cost, assumed	EUR 180/m^2	EUR 180/m^2
Access allocation, assumed	EUR 15,000	EUR 60,000
Downtime cost, assumed	EUR 10,000	EUR 30,000
Inspection at year 4, assumed	EUR 5000; 200 kg CO_2e	EUR 5000; 200 kg CO_2e
Allocated vessel fuel, assumed	500 L	2000 L
Climate factors, assumed	12 kg CO_2e/m^2 repair; 3.2 kg CO_2e/L fuel	Same factors
Incremental present-value cost, calculated	EUR 41,276.85	EUR 104,852.07
Incremental climate impact, calculated	2648.53 kg CO_2e total; 2.65 kg CO_2e/m^2 protected	7800 kg CO_2e total; 7.80 kg CO_2e/m^2 protected
Post-repair fraction at year 8, calculated	0.01414	0.01000

6.4.1. Condition History and Remaining Protective Life

Let f be the mapped fraction of coating area affected by a consistently defined defect or delamination criterion. Assume f = 0.01, 0.02, and 0.04 at years 0, 2, and 4, respectively.

Year 0 is an inspection baseline with existing defects, not necessarily the date of coating application. A local exponential model gives $k = [\ln(0.04) - \ln(0.01)]/4 = 0.3466\ \text{year}^{-1}$. The three assumed points lie exactly on this curve, so this calculation demonstrates parameter estimation but supplies no estimate of measurement error or field scatter. The model is used only below the specified intervention threshold; it is not valid as an unbounded long-term area-growth law:

$$f(t) = f_4 \exp[k(t - 4)] \quad (2)$$

For an assumed protective-function limit $f_{lim} = 0.10$, the remaining protective life at year 4 is obtained from Equation (3). This threshold is a demonstration choice, not a recommended allowable damaged area. A structural metal-loss limit must be assessed separately and could require an earlier intervention:

$$RUL_4 = \ln(f_{lim}/f_4)/k = 2.64\ \text{years} \quad (3)$$

The central threshold is therefore reached at year 6.64 without repair. Assumed rates of 0.25 and 0.45 year^{-1} give RUL values of 3.67 and 2.04 years, respectively; these are sensitivity cases, not a confidence interval. At fixed k, changing f_4 from 0.035 to 0.045 gives RUL values of 3.03 and 2.30 years. This second calculation illustrates measurement sensitivity without assigning an unsupported probability distribution. In practice, repeated mapped observations and withheld field data would be needed to estimate variability and test prediction coverage.

6.4.2. Repair Area and Incremental Lifecycle Cost

Compare a planned shared campaign at year 5 with a dedicated campaign at year 6. Their central affected fractions are 0.05657 and 0.08000. Applying an overlap factor $\alpha = 1.25$ to the mapped affected area gives the prepared and recoated area A_r in Equation (4). Areas are assumed non-overlapping; an asset calculation should instead use mapped repair polygons and avoid counting shared overlap twice:

$$A_r(t_r) = \alpha\ A\ f(t_r) \quad (4)$$

Assume a repair unit cost c_r of EUR 180/m^2, a current inspection cost C_I of EUR 5000, and a real annual discount rate r of 4%. The year-5 strategy allocates EUR 15,000 of shared access cost and EUR 10,000 of downtime; the year-6 strategy assumes EUR 60,000 for dedicated access and EUR 30,000 for downtime. These are scenario inputs, not offshore market estimates. Equation (5) discounts each intervention to the year-4 decision date. The common initial coating cost is already incurred and cancels from this incremental comparison:

$$PV = C_I + [C_M + c_r\ A_r(t_r) + C_D]/(1 + r)^{t_r - 4} \quad (5)$$

Here, C_M is allocated mobilization/access cost and C_D is downtime cost. The resulting present values are EUR 41,276.85 for year-5 repair and EUR 104,852.07 for year-6 repair. This difference is driven by the assumed campaign logistics as well as defect growth; it is not an observed saving attributable to a coating formulation. If the later strategy receives the same EUR 15,000 access allocation and EUR 10,000 downtime assumption, its present value becomes EUR 44,755.92, narrowing the difference to EUR 3479.07. Shared vessel burdens must be allocated consistently, not counted as a full mobilization for every repaired region.

For a common service comparison, assume inspection confirms an aggregate residual affected fraction of 0.005 immediately after either repair and the same subsequent k. The predicted year-8 fractions are 0.01414 after year-5 repair and 0.01000 after year-6 repair, both

below 0.10. This aggregate reset is an explicit simplifying assumption: only treated regions are repaired, and the previously sound coating is not made new. No further campaign, steel replacement, or residual asset value is included within this four-year horizon. If post-repair adhesion or substrate condition does not meet acceptance criteria, the common-service assumption fails and further intervention burdens must be added.

6.4.3. Climate Inventory and Decision Sensitivity

To demonstrate one environmental impact category, assume 12 kg CO_2e per repaired square metre for the combined preparation, coating, application, removal, and waste processes. Also assume allocated vessel fuel of 500 L for the shared campaign or 2000 L for the dedicated campaign, a fuel factor of 3.2 kg CO_2e/L, and a common inspection burden G_I of 200 kg CO_2e. Each factor is illustrative and would need to be replaced by a documented inventory and consistent upstream/combustion boundary. Equation (6) calculates undiscounted climate impact; financial discounting is not applied to physical emissions:

$$G = G_I + g_r A_r + g_F F \quad (6)$$

In Equation (6), g_r is the repair-area factor, g_F is the fuel factor, and F is allocated fuel volume. Normalizing by the 1000 m^2 protected region gives 2.65 and 7.80 kg CO_2e/m^2 over years 4–8, respectively. The repair-area denominator is not used for this functional comparison. Initial construction, identical background activities, end-of-life treatment outside the horizon, and avoided steel replacement are excluded from both strategies. This is an incremental climate-impact illustration within an LCA framework, not a complete multi-category LCA or evidence of low aquatic toxicity. A full assessment must also quantify resource use, marine releases, toxicity, and any strategy-dependent changes outside this boundary.

The access screen can alter the apparent economic choice. At k = 0.45 $year^{-1}$, the year-6 campaign plus a 0.5-year delay occurs 2.5 years after the decision, exceeding the 2.04-year protective life. The year-5 campaign plus the same delay occurs after 1.5 years and remains within that scenario limit. An ineffective repair that leaves f = 0.02, instead of 0.005, would also reduce the central post-repair time to the 0.10 limit from 8.64 to 4.64 years. These sensitivity cases show why access, hidden damage, and repair effectiveness must accompany a mean RUL. They do not quantify failure probability, which requires measured variability and a validated probabilistic model.

Figure 4 shows the entire calculation: assumed condition observations determine k and the threshold-crossing time; the chosen intervention date sets repair area; that same area enters the discounted cost and climate inventory. The shaded range in Figure 4a contains alternative growth-rate scenarios, not confidence bounds. Figure 4b,c compares the stated logistics assumptions and system boundaries. Operational use would require independent validation of defect mapping, the growth law, the threshold, post-repair response, and every cost and emission factor.

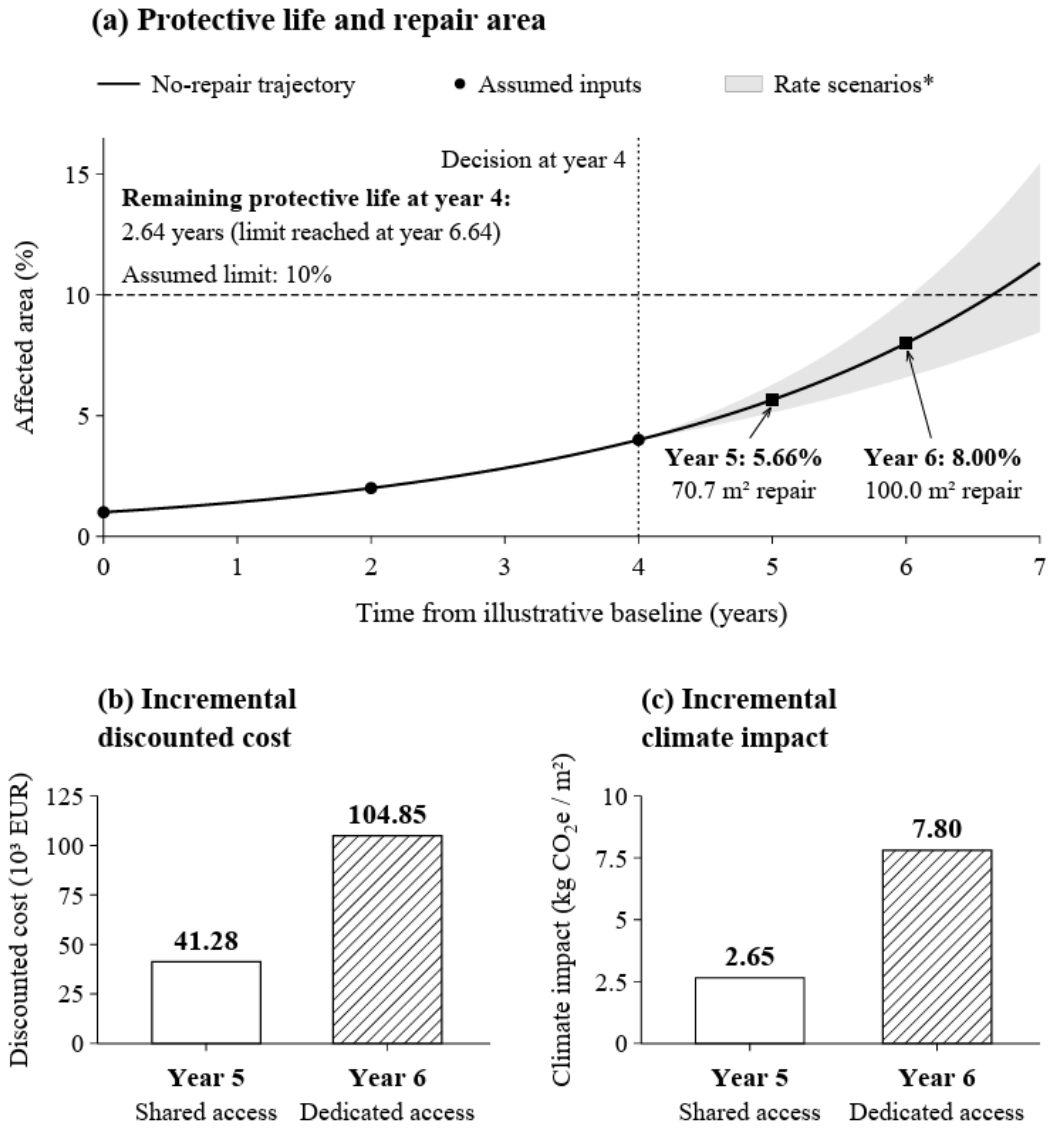


Figure 4. Illustrative link from coating condition to intervention outcomes. (**a**) Assumed affected-area inputs, central no-repair trajectory, and growth-rate scenarios. Markers at years 5 and 6 identify alternative repair times; the plotted trajectory is not the post-repair history. (**b**) Incremental intervention cost discounted to year 4. (**c**) Incremental climate impact per square metre protected over years 4–8.

7. Conclusions and Future Perspectives

The preferred near-term approach for ORE steel is a zone-specific, redundant protection system established during fabrication. For atmospheric steel, the reference option is a qualified anticorrosive primer and epoxy barrier with a weather-resistant outer coat. For difficult-access splash/tidal steel, this critical narrative review gives priority to qualified high-build epoxy or metallic–organic duplex systems with demonstrated wet adhesion, edge coverage, and damage tolerance. Where metallization and compatible overcoats can be applied reproducibly, the field evidence makes duplex protection a strong candidate for long intervals between repairs; it does not prove that every duplex formulation is superior at every site.

For permanently immersed steel, the preferred architecture combines a qualified immersion barrier with cathodic protection designed for realistic defect growth and coating breakdown. TSA is an alternative where its composition, consumption, sealing, electrical continuity, and compatibility with the full protection system are established. Foul-release layers are justified where fouling compromises performance and release or cleaning

forces are available. Tidal blades and exposed wear regions need locally qualified erosion/cavitation protection, while highly strained components require measured strain tolerance; rigid ceramic layers and soft foul-release films should not be extrapolated across these duties.

Nanocomposite formulations should advance when dispersion and interfacial chemistry improve that limiting mechanism at matched thickness and cure. Self-healing and sensing additives are currently better treated as supplemental functions than as the primary defense of inaccessible steel. The decisive demonstrations are recovery of corrosion protection in seawater after representative damage, retention after repeated events, and an observable response under fouling and actual access conditions. Finite inhibitor inventory, chain-mobility requirements, and the need for externally supplied heat or light can prevent a successful laboratory concept from functioning underwater.

The preferred system combines controlled preparation, a field-supported barrier or duplex architecture, cathodic protection where applicable, and additional functions justified by component duty. The worked example shows how a common damage history can determine RUL, repair area, cost, and climate inventory. Its sensitivity to growth rate and access illustrates the required decision logic, while its assumed parameters prevent extrapolation to an operating asset. Coating-condition forecasts become useful engineering inputs only after calibration and independent validation.

The next development step is a direct comparison of such reference architectures with advanced candidates using the controlled combined-stressor schemes proposed in Table 4, followed by matched offshore exposure. Evidence that would change the present preference is a reproducible reduction in wet defect growth or repair demand without compromising application quality, environmental performance, or reparability. Until then, established protection with measurable damage tolerance and planned maintenance access is the more defensible engineering choice than an unvalidated coating that combines many nominal functions.

The evidence gaps are specific: matched offshore trials of advanced versus qualified reference systems; fatigue and wear tests that track coating damage together with substrate corrosion; product-level environmental data during cleaning and erosion; and repair histories long enough to calibrate protective-life forecasts. The immediate research preference is to close those gaps with shared exposure records and prespecified failure criteria. An improvement in laboratory impedance, tensile healing, or contact angle should change engineering practice only when it improves the relevant field endpoint without sacrificing adhesion, repairability, or environmental performance.

Funding: This research was funded by Korea SMEs and Startups Agency, grant number G0900002616.

Institutional Review Board Statement: Not applicable.

Informed Consent Statement: Not applicable.

Data Availability Statement: No new data were created or analyzed in this study. Data sharing is not applicable to this article.

Conflicts of Interest: The author declares no conflicts of interest.

Abbreviations

The following abbreviations are used in this manuscript:

ORE	offshore renewable energy
UV	ultraviolet
MIC	microbiologically influenced corrosion

TSA	thermally sprayed aluminum
EIS	electrochemical impedance spectroscopy
NDT	non-destructive testing
RUL	remaining useful life
LCA	Lifecycle assessment
LCC	lifecycle cost
CP	cathodic protection
PU	polyurethane
PDMS	polydimethylsiloxane

References

1. Price, S.J.; Figueira, R.B. Corrosion protection systems and fatigue corrosion in offshore wind structures: Current status and future perspectives. *Coatings* **2017**, *7*, 25. [CrossRef]
2. DNV. *DNV-RP-0416: Corrosion Protection for Wind Turbines*; Amended 2021; DNV: Høvik, Norway, 2016. Available online: https://www.dnv.com/energy/standards-guidelines/dnv-rp-0416-corrosion-protection-for-wind-turbines/ (accessed on 21 September 2026).
3. Portas, A.; Briand, J.-F.; Damblans, G.; Quillien, N. A review of biofouling characteristics and issues for offshore renewable energy industry. *Biofouling* **2026**, *42*, 339–360. [CrossRef] [PubMed]
4. Eom, S.-H.; Kim, S.-S.; Lee, J.-B. Assessment of anti-corrosion performances of coating systems for corrosion prevention of offshore wind power steel structures. *Coatings* **2020**, *10*, 970. [CrossRef]
5. Xu, C.; Liu, W. Organic–inorganic hybrid corrosion protection coating materials for offshore wind power devices: A mini-review and perspective. *Mol. Cryst. Liq. Cryst.* **2020**, *710*, 74–89. [CrossRef]
6. Kirchgeorg, T.; Weinberg, I.; Hörnig, M.; Baier, R.; Schmid, M.J.; Brockmeyer, B. Emissions from corrosion protection systems of offshore wind farms: Evaluation of the potential impact on the marine environment. *Mar. Pollut. Bull.* **2018**, *136*, 257–268. [CrossRef] [PubMed]
7. *ISO 12944-9:2018*; Paints and Varnishes—Corrosion Protection of Steel Structures by Protective Paint Systems—Part 9: Protective Paint Systems and Laboratory Performance Test Methods for Offshore and Related Structures. ISO: Geneva, Switzerland, 2018. Available online: https://www.iso.org/standard/64832.html (accessed on 21 September 2026).
8. Brijder, R.; Hagen, C.H.M.; Cortés, A.; Irizar, A.; Thibbotuwa, U.C.; Helsen, S.; Vásquez, S.; Ompusunggu, A.P. Review of corrosion monitoring and prognostics in offshore wind turbine structures: Current status and feasible approaches. *Front. Energy Res.* **2022**, *10*, 991343. [CrossRef]
9. Grinon-Echaniz, R.; Paul, S.; Thornton, R.; Refait, P.; Jeannin, M.; Rodriguez, A. Prediction of thermal spray coatings performance in marine environments by combination of laboratory and field tests. *Coatings* **2021**, *11*, 320. [CrossRef]
10. Marinova, N.; Urbegain, A.; Benguria, P.; Travé, A.; Caracena, R. Evaluation of anticorrosion coatings for offshore wind turbine monopiles for an optimized and time-efficient coating application. *Coatings* **2022**, *12*, 384. [CrossRef]
11. Maduka, M.; Schoefs, F.; Thiagarajan, K.; Bates, A. Hydrodynamic effects of biofouling-induced surface roughness—Review and research gaps for shallow water offshore wind energy structures. *Ocean Eng.* **2023**, *272*, 113798. [CrossRef]
12. Jin, J.; Li, Y.; Huang, H.; Xiang, Y.; Yan, W. Symbiosis of sulfate-reducing bacteria and total general bacteria affects microbiologically influenced corrosion of carbon steel. *Coatings* **2024**, *14*, 788. [CrossRef]
13. Wakai, S.; Eno, N.; Mizukami, H.; Sunaba, T.; Miyanaga, K.; Miyano, Y. Microbiologically influenced corrosion of stainless steel independent of sulfate-reducing bacteria. *Front. Microbiol.* **2022**, *13*, 982047. [CrossRef] [PubMed]
14. Kumar, R. Tribological challenges in ocean energy systems: Failure mechanisms, materials, lubrication strategies, and reliability roadmaps. *Results Surf. Interfaces* **2026**, *23*, 100750. [CrossRef]
15. E, R.; Li, H.; Li, Y.; Li, Y. Research progress on aging test and performance evaluation of marine coatings. *Polym. Degrad. Stab.* **2025**, *241*, 111614. [CrossRef]
16. López-Ortega, A.; Arana, J.L.; Rodríguez, E.; Bayón, R. Corrosion, wear and tribocorrosion performance of a thermally sprayed aluminum coating modified by plasma electrolytic oxidation technique for offshore submerged components protection. *Corros. Sci.* **2018**, *143*, 258–280. [CrossRef]
17. Xu, Y.; Zhang, Q.; Zhou, Q.; Gao, S.; Wang, B.; Wang, X.; Huang, Y. Flow accelerated corrosion and erosion−corrosion behavior of marine carbon steel in natural seawater. *npj Mater. Degrad.* **2021**, *5*, 56. [CrossRef]
18. Zhang, X.; Huang, Z.; Wang, K.; Wang, J.; Zammit, A.; Buhagiar, J.; Cassar, G.; Liu, M.; Chen, J. Erosion-corrosion behavior and mechanism of TiAlN coating under different flow conditions in simulated seawater. *Corrosion* **2023**, *79*, 615–623. [CrossRef] [PubMed]

19. Lee, J.H.; Kim, J.H.; Kim, Y.P.; Kim, S.J. Evaluation of anti-cavitation performance of polyurethane coatings in seawater using ultrasonic vibratory method. *J. Weld. Join.* **2019**, *37*, 455–462. [CrossRef]
20. Momber, A.W.; Plagemann, P.; Stenzel, V. Performance and integrity of protective coating systems for offshore wind power structures after three years under offshore site conditions. *Renew. Energy* **2015**, *74*, 606–617. [CrossRef]
21. Momber, A.W.; Marquardt, T.; Irmer, M.; Kelm, D. Effects of compressive damage on the corrosion protection performance of offshore wind power coating systems. *Mater. Corros.* **2025**, *76*, 887–895. [CrossRef]
22. Zhang, H.; Huang, X.; Yang, L.; Chen, X.; Lu, J. Experimental study and finite element analysis of degradation behavior of epoxy zinc-rich coating system under stress corrosion. *J. Adhes. Sci. Technol.* **2024**, *38*, 618–636. [CrossRef]
23. *ASTM G8-24*; Standard Test Methods for Cathodic Disbonding of Coated Steel. ASTM International: West Conshohocken, PA, USA, 2024. [CrossRef]
24. *ASTM G119-09(2021)*; Standard Guide for Determining Synergism Between Wear and Corrosion. ASTM International: West Conshohocken, PA, USA, 2021. [CrossRef]
25. Larsson, A.I.; Mattsson-Thorngren, L.; Granhag, L.M.; Berglin, M. Fouling-release of barnacles from a boat hull with comparison to laboratory data of attachment strength. *J. Exp. Mar. Biol. Ecol.* **2010**, *392*, 107–114. [CrossRef]
26. Lagerström, M.; Wrange, A.L.; Oliveira, D.R.; Granhag, L.; Larsson, A.I.; Ytreberg, E. Are silicone foul-release coatings a viable and environmentally sustainable alternative to biocidal antifouling coatings in the Baltic Sea region? *Mar. Pollut. Bull.* **2022**, *184*, 114102. [CrossRef] [PubMed]
27. Wang, D.; Wang, Y.; Cai, Y.; Qiu, L. Polyaniline/ZrO_2 doped epoxy nanocomposite coatings with synergistic maze-passivation and hydrophobicity for marine anticorrosion and antifouling. *Prog. Org. Coat.* **2026**, *216*, 110199. [CrossRef]
28. Zhou, A.; Yu, H.; Tang, J.; Zhang, B.; Qi, F.; Zhou, Y.; Zhao, N.; Ouyang, X. N-PMI modified PAZ nanocomposite coatings with self-healing function for anticorrosion and antifouling applications. *Prog. Org. Coat.* **2023**, *180*, 107589. [CrossRef]
29. Fan, B.; Yang, J.; Cao, L.; Wang, X.; Li, J.; Yang, Y.; Wang, Q.; Zhang, P.; Vogel, F.; Li, W.; et al. Revealing the impact of micro-SiO2 filer content on the anti-corrosion performance of water-borne epoxy resin. *Polymers* **2023**, *15*, 3273. [CrossRef] [PubMed]
30. Cui, Y.-Y.; Sheng, M.-Q.; Liu, Y.; Feng, Y.; Li, H.-J.; Wu, Y.-C. Antifouling and self-healing performance of marine coatings based on hydrogen-bond interactions. *ACS Appl. Mater. Interfaces* **2023**, *15*, 58967–58975. [CrossRef] [PubMed]
31. Shchukin, D.G.; Zheludkevich, M.; Yasakau, K.; Lamaka, S.; Ferreira, M.G.S.; Möhwald, H. Layer-by-layer assembled nanocontainers for self-healing corrosion protection. *Adv. Mater.* **2006**, *18*, 1672–1678. [CrossRef]
32. Qian, B.; Zheng, Z.; Michailids, M.; Fleck, N.; Bilton, M.; Song, Y.; Li, G.; Shchukin, D. Mussel-inspired self-healing coatings based on polydopamine-coated nanocontainers for corrosion protection. *ACS Appl. Mater. Interfaces* **2019**, *11*, 10283–10291. [CrossRef] [PubMed]
33. Syrek-Gerstenkorn, B.; Paul, S. Metallic coatings in offshore wind sector—A mini review. *npj Mater. Degrad.* **2024**, *8*, 86. [CrossRef]
34. Paul, S. Effect of damage on the corrosion performance of thermal spray aluminium (TSA) coating in synthetic seawater. *Appl. Sci.* **2023**, *13*, 1109. [CrossRef]
35. Matikainen, V.; Niemi, K.; Koivuluoto, H.; Vuoristo, P. Abrasion, erosion and cavitation erosion wear properties of thermally sprayed alumina based coatings. *Coatings* **2014**, *4*, 18–36. [CrossRef]
36. Qiao, X.; Chen, R.; Zhang, H.; Liu, J.; Liu, Q.; Yu, J.; Liu, P.; Wang, J. Outstanding cavitation erosion resistance of hydrophobic polydimethylsiloxane-based polyurethane coatings. *J. Appl. Polym. Sci.* **2019**, *136*, 47668. [CrossRef]
37. Wang, C.; Hou, S.; Wang, J.; Liu, Y.; Su, Y.; Fan, W.; Li, M. A multifunctional smart coating with damage visual warning, self-healing, antibacterial, and long-term anti-corrosion properties for marine applications. *ACS Appl. Polym. Mater.* **2026**, *8*, 7418–7437. [CrossRef]
38. Wang, J.-P.; Song, X.; Wang, J.-K.; Cui, X.; Zhou, Q.; Qi, T.; Li, G.L. Smart-sensing polymer coatings with autonomously reporting corrosion dynamics of self-healing systems. *Adv. Mater. Interfaces* **2019**, *6*, 1900055. [CrossRef]
39. Zhang, J.; Frankel, G.S. Corrosion-sensing behavior of an acrylic-based coating system. *Corrosion* **1999**, *55*, 957–967. [CrossRef]
40. Schumacher, J.F.; Carman, M.L.; Estes, T.G.; Feinberg, A.W.; Wilson, L.H.; Callow, M.E.; Callow, J.A.; Finlay, J.A.; Brennan, A.B. Engineered antifouling microtopographies—Effect of feature size, geometry, and roughness on settlement of zoospores of the green alga Ulva. *Biofouling* **2007**, *23*, 55–62. [CrossRef] [PubMed]
41. Momber, A.W.; Marquardt, T.; Buchbach, S.; Plagemann, P. The corrosion protection performance of repair coatings for offshore wind power constructions after long-term splash zone site exposure. *Mater. Corros.* **2022**, *73*, 526–539. [CrossRef]
42. Momber, A.W.; Plagemann, P.; Stenzel, V. The adhesion of corrosion protection coating systems for offshore wind power constructions after three years under offshore exposure. *Int. J. Adhes. Adhes.* **2016**, *65*, 96–101. [CrossRef]
43. *ISO 8501-1:2007*; Preparation of Steel Substrates Before Application of Paints and Related Products—Visual Assessment of Surface Cleanliness—Part 1: Rust Grades and Preparation Grades of Uncoated Steel Substrates and of Steel Substrates After Overall Removal of Previous Coatings. ISO: Geneva, Switzerland, 2007. Available online: https://www.iso.org/standard/43426.html (accessed on 21 September 2026).

44. Pélissier, K.; Le Bozec, N.; Thierry, D.; Larché, N. Evaluation of the long-term performance of marine and offshore coatings system exposed on a traditional stationary site and an operating ship and its correlation to accelerated test. *Coatings* **2022**, *12*, 1758. [CrossRef]
45. *ISO 8503-1:2012*; Preparation of Steel Substrates Before Application of Paints and Related Products—Surface Roughness Characteristics of Blast-Cleaned Steel Substrates—Part 1: Specifications and Definitions for ISO Surface Profile Comparators for the Assessment of Abrasive Blast-Cleaned Surfaces. ISO: Geneva, Switzerland, 2012. Available online: https://www.iso.org/standard/51979.html (accessed on 21 September 2026).
46. Momber, A.W.; Buchbach, S.; Plagemann, P.; Marquardt, T.; Winkels, I.; Viertel, J. Statistical effects of surface preparation and coating type on the corrosion protection performance of repair coatings for offshore wind power constructions. *Mater. Corros.* **2018**, *69*, 460–471. [CrossRef]
47. *ASTM D4541-22*; Standard Test Method for Pull-Off Strength of Coatings Using Portable Adhesion Testers. ASTM International: West Conshohocken, PA, USA, 2022. [CrossRef]
48. McIntyre, J.M.; Pham, H.Q. Electrochemical impedance spectroscopy; a tool for organic coatings optimizations. *Prog. Org. Coat.* **1996**, *27*, 201–207. [CrossRef]
49. Bongiorno, V.; Michailidou, E.; Curioni, M. Evaluating organic coating performance by EIS: Correlation between long-term EIS measurements and corrosion of the metal substrate. *Mater. Corros.* **2024**, *75*, 156–173. [CrossRef]
50. Juhl, M.; Hauschild, M.Z.; Dam-Johansen, K. Sustainability of corrosion protection for offshore wind turbine towers. *Prog. Org. Coat.* **2024**, *186*, 107998. [CrossRef]
51. Demirel, Y.K.; Uzun, D.; Zhang, Y.; Turan, O. Life cycle assessment of marine coatings applied to ship hulls. In *Trends and Challenges in Maritime Energy Management*; Ölçer, A.I., Kitada, M., Dalaklis, D., Ballini, F., Eds.; WMU Studies in Maritime Affairs, Volume 6; Springer: Cham, Switzerland, 2018; pp. 325–339. [CrossRef]
52. *ASTM B117-19*; Standard Practice for Operating Salt Spray (Fog) Apparatus. ASTM International: West Conshohocken, PA, USA, 2019. [CrossRef]
53. *ASTM D4060-19*; Standard Test Method for Abrasion Resistance of Organic Coatings by the Taber Abraser. ASTM International: West Conshohocken, PA, USA, 2019. [CrossRef]
54. *ASTM D3363-22*; Standard Test Method for Film Hardness by Pencil Test. ASTM International: West Conshohocken, PA, USA, 2022. [CrossRef]
55. *ASTM D2240-15(2021)*; Standard Test Method for Rubber Property—Durometer Hardness. ASTM International: West Conshohocken, PA, USA, 2021. [CrossRef]
56. *ASTM D2794-93(2024)*; Standard Test Method for Resistance of Organic Coatings to the Effects of Rapid Deformation (Impact). ASTM International: West Conshohocken, PA, USA, 2024. [CrossRef]
57. *ASTM D522/D522M-17(2021)*; Standard Test Methods for Mandrel Bend Test of Attached Organic Coatings. ASTM International: West Conshohocken, PA, USA, 2021. [CrossRef]
58. *ASTM D570-22*; Standard Test Method for Water Absorption of Plastics. ASTM International: West Conshohocken, PA, USA, 2022. [CrossRef]
59. *ASTM D5894-21*; Standard Practice for Cyclic Salt Fog/UV Exposure of Painted Metal (Alternating Exposures in a Fog/Dry Cabinet and a UV/Condensation Cabinet). ASTM International: West Conshohocken, PA, USA, 2021. [CrossRef]
60. Mehmanparast, A.; Vidament, A. An accelerated corrosion-fatigue testing methodology for offshore wind applications. *Eng. Struct.* **2021**, *240*, 112414. [CrossRef]
61. Ren, Z.; Verma, A.S.; Li, Y.; Teuwen, J.J.E.; Jiang, Z. Offshore wind turbine operations and maintenance: A state-of-the-art review. *Renew. Sustain. Energy Rev.* **2021**, *144*, 110886. [CrossRef]
62. Pacheco-Blazquez, R.; Garcia-Espinosa, J.; Di Capua, D.; Pastor Sanchez, A. A digital twin for assessing the remaining useful life of offshore wind turbine structures. *J. Mar. Sci. Eng.* **2024**, *12*, 573. [CrossRef]
63. McMorland, J.; Collu, M.; McMillan, D.; Carroll, J. Operation and maintenance for floating wind turbines: A review. *Renew. Sustain. Energy Rev.* **2022**, *163*, 112499. [CrossRef]
64. Tusar, M.I.H.; Sarker, B.R. Maintenance cost minimization models for offshore wind farms: A systematic and critical review. *Int. J. Energy Res.* **2022**, *46*, 3739–3765. [CrossRef]
65. Deb, K.; Pratap, A.; Agarwal, S.; Meyarivan, T. A fast and elitist multiobjective genetic algorithm: NSGA-II. *IEEE Trans. Evol. Comput.* **2002**, *6*, 182–197. [CrossRef]

Disclaimer/Publisher's Note: The statements, opinions and data contained in all publications are solely those of the individual author(s) and contributor(s) and not of MDPI and/or the editor(s). MDPI and/or the editor(s) disclaim responsibility for any injury to people or property resulting from any ideas, methods, instructions or products referred to in the content.